Stem Cell Reports
Article

ISSCR

OPEN ACCESS

Chemical Conversion of Human Fetal Astrocytes into Neurons through Modulation of Multiple Signaling Pathways

Jiu-Chao Yin,[1,2] Lei Zhang,[1,2] Ning-Xin Ma,[1] Yue Wang,[1] Grace Lee,[1] Xiao-Yi Hou,[1] Zhuo-Fan Lei,[1] Feng-Yu Zhang,[1] Feng-Ping Dong,[1] Gang-Yi Wu,[1] and Gong Chen[1,*]

[1]Department of Biology, Huck Institutes of Life Sciences, Pennsylvania State University, University Park, PA 16802, USA

[2]Co-first author

*Correspondence: gongchen@psu.edu or http://bio.psu.edu/directory/guc2 (G.C.)

https://doi.org/10.1016/j.stemcr.2019.01.003

SUMMARY

We have previously developed a cocktail of nine small molecules to convert human fetal astrocytes into neurons, but a nine-molecule recipe is difficult for clinical applications. Here, we identify a chemical formula with only three to four small molecules for astrocyte-to-neuron conversion. We demonstrate that modulation of three to four signaling pathways among Notch, glycogen synthase kinase 3, transforming growth factor β, and bone morphogenetic protein pathways is sufficient to change an astrocyte into a neuron. The chemically converted human neurons can survive >7 months in culture, fire repetitive action potentials, and display robust synaptic burst activities. Interestingly, cortical astrocyte-converted neurons are mostly glutamatergic, while midbrain astrocyte-converted neurons can yield some GABAergic neurons in addition to glutamatergic neurons. When administered *in vivo* through intracranial or intraperitoneal injection, the four-drug combination can significantly increase adult hippocampal neurogenesis. Together, human fetal astrocytes can be chemically converted into functional neurons using three to four small molecules, bringing us one step forward for developing future drug therapy.

INTRODUCTION

Neuronal loss is the leading cause of symptoms in patients with neural injury or neurodegenerative disorders. Following nerve injury, glial cells including astrocytes, NG2 cells, and microglia will proliferate and become reactive glial cells to form glial scarring in order to protect neighboring tissues from further damage (Burda and Sofroniew, 2014). However, the continuous presence of glial scars also inhibits neuronal growth and synaptic transmission in the injured area (Filous and Silver, 2016; Yiu and He, 2006). Thus, reactive glial cells are a double-edged sword that can have both neuroprotective and neuroinhibitory functions during the progression of injury or diseases. Glial scarring has been widely reported after traumatic brain injury, stroke, and spinal cord injury, but efforts to remove the neuroinhibitory effect of glial scarring has only resulted in limited success (Filous and Silver, 2016; Pekny and Nilsson, 2005).

We have recently demonstrated that reactive astrocytes and NG2 cells can be directly reprogrammed into functional neurons inside mouse brains with the expression of a single neural transcription factor, NEUROD1 (Guo et al., 2014). Other transcription factors, such as neurogenin 2 (NGN2), ASCL1, and SOX2, have also been reported to reprogram glial cells into neurons both *in vitro* and *in vivo* (Berninger et al., 2007; Grande et al., 2013; Heinrich et al., 2010; Liu et al., 2015; Niu et al., 2013; Su et al., 2014; Torper et al., 2015). Direct conversion from glial cells into neurons inside the brain or spinal cord without cell transplantation can avoid the problems of tumor formation, aberrant differentiation, and immunorejection that are often associated with stem cell transplantation (Li and Chen, 2016). The majority of glia-to-neuron conversion research has been carried out using virus-mediated ectopic expression of transcription factors, which requires production of viruses and sophisticated intracranial or intra-spinal injection procedures. However, small-molecule-mediated chemical reprogramming has been developed to allow cell transdifferentiation without viruses (Cao et al., 2016; Cheng et al., 2014; Hu et al., 2015; Li et al., 2015; Zhang et al., 2015, 2016a; Zhao et al., 2015). Our lab recently developed a chemical protocol to reprogram human astrocytes (HAs) into functional neurons using a cocktail of nine small molecules (Zhang et al., 2015). These nine molecules need to be sequentially administered to reprogram HAs into neurons, making its clinical translation quite difficult due to the large number of small molecules used and the complicated timing of drug application.

In this study, we identify a chemical protocol composed of only three to four small molecules (DAPT, CHIR99021, SB431542, and LDN193189) that can more efficiently reprogram HAs into neurons. By substituting each of these four drugs (core drugs) with functional analogs, we demonstrate that simultaneous modulation of four signaling pathways including Notch, glycogen synthase kinase 3β (GSK-3β), transforming growth factor β (TGF-β), and bone morphogenetic protein (BMP) pathways, is sufficient to reprogram HAs into neurons. Even modulating three out of the four signaling pathways can convert HAs into

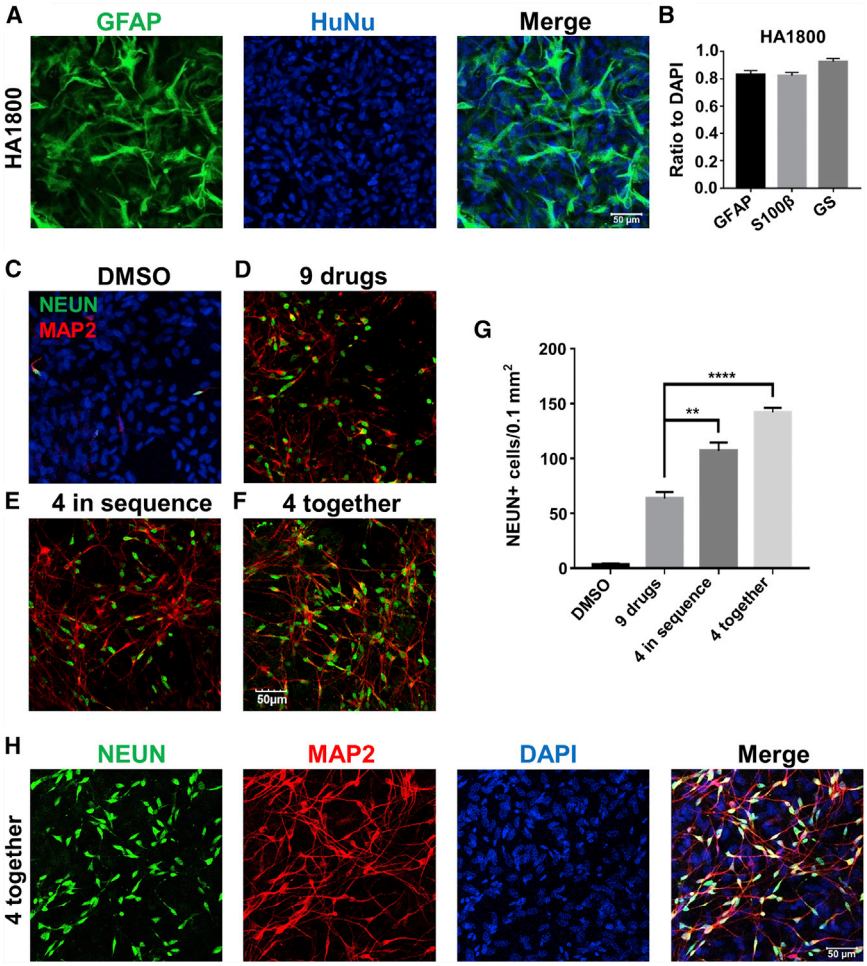

Figure 1. Identification of Four Core Drugs to Chemically Reprogram HA into Neurons

(A) HA (1800, ScienCell) were characterized by immunostaining of astrocyte marker GFAP (green) and human nuclei (HuNu).

(B) Quantified data showing the majority of cells immunopositive for astrocyte markers (GFAP+, 84.7% ± 2.7%; S100β+, 82.3% ± 2.3%; glutamine synthetase [GS]+, 92.5% ± 2.5%). N = 3 batches.

(C) HA treated with 0.2% DMSO had few neurons when assessed with neuronal markers NEUN (green) and MAP2 (red).

(D) Sequential application of a nine-drug cocktail for 8 days resulted in a significant number of neurons as described recently (Zhang et al., 2015).

(E and F) The four core drugs (DAPT, CHIR99021, SB431542, and LDN193189) were administered either in sequence (E) or together (F) for 6 days, and both yielded a significant number of neurons.

(G) Quantified data (NEUN) showing higher reprogramming efficiency when four drugs (DCSL) were added in sequence or together as a mixture. $^{**}p < 0.01$, $^{****}p < 0.0001$, one-way ANOVA followed with Dunnett's multiple comparison test. Data are represented in means ± SEM. The immunostaining was performed at 14 days after the beginning of drug treatment. N = 3 batches.

(H) Representative images of neurons converted by four drugs together at day 14. Neurons were labeled by NEUN (green) and MAP2 (red), while DAPI (blue) showed all cell nuclei. Scale bars, 50 μm.

neurons. Our chemically converted human neurons are highly functional and can survive >7 mo in cell culture. Moreover, when applied *in vivo*, core drugs significantly increase the adult neurogenesis in the mouse hippocampus. Therefore, we have identified a simple chemical formula for astrocyte-to-neuron conversion, bringing us one step closer toward developing future drug therapy for brain repair.

RESULT

Identification of Four Core Drugs for Astrocyte-to-Neuron Conversion

We have recently identified a combination of nine small molecules, including SB431542, LDN193189, TTNPB, Thiazovivin, CHIR99021, DAPT, valproic acid (VPA), smoothened agonist (SAG), and purmorphamine (Purmo), to reprogram human fetal astrocytes into functional neurons (Zhang et al., 2015). However, for therapeutic purpose, a nine-molecule cocktail added in a sequential manner is rather difficult to translate into clinical applications. Here, to search for a more practical formula for chemical reprogramming, we purchased human fetal astrocytes (HA1800) from ScienCell (San Diego, CA) as described previously (Zhang et al., 2015). Because human fetal astrocytes might contain neuroprogenitors, we have subcultured the astrocytes for at least ten generations in the presence of 10% fetal bovine serum (FBS) to minimize progenitors (Zhang et al., 2015). After more than ten passages, the majority of our astrocytes were immunopositive for astrocytic markers such as glial fibrillary acidic protein(GFAP), S100β, and glutamine synthetase (Figures 1A, 1B, and S1A), but rarely for neuroprogenitor markers SOX2 (Figures S1B and S1C) and NESTIN (Figures S2E and S2F). Long-term culture of our HAs in neural differentiation medium for

1 month also rarely yielded any neurons (Figures S1D and S1E). At the transcriptome level (Figure S1F), in comparison with published datasets on HAs (Zhang et al., 2016b) or human neural stem cells (hNSCs) (Modrek et al., 2017), our HA samples (red box, GSE123397) were closely related to the fetal astrocytes from human brain, but clearly different from the hNSCs (green box). Figure S1G shows the heatmap of gene expression of typical astrocyte and NSC markers. Our HA samples showed low expression of *STMN1*, *DLX1*, and *NES* but high expression of *FN1*, *COL1A1*, *VIM*, and *MYC*, which was opposite to that of hNSCs. Together, the significant difference between our HA samples and NSCs suggests that after ten passages in 10% FBS, neuroprogenitors are minimized in our HA cultures.

After characterizing HA properties, we repeated and confirmed successful chemical conversion of HAs into neurons using the nine-molecule cocktail (Zhang et al., 2015) (Figures 1C and 1D). We then investigated how to reduce the number of drugs for chemical reprogramming by studying the effect of each individual drug among the nine-molecule cocktail. Interestingly, four molecules including SB431542 (S), LDN193189 (L), CHIR99021 (C), and DAPT (D) appeared to be most critical in maintaining high reprogramming efficiency (Zhang et al., 2015). Therefore, we tested these four drugs (SLCD) together to determine their reprogramming capability. Unexpectedly, when we applied SB431542 (5 μM) and LDN193189 (0.25 μM) for 2 days, and then replaced with CHIR99021 (1.5 μM) and DAPT (5 μM) for 4 days, it yielded more neurons than the nine-drug formula (Figures 1E and 1G). When we applied the four drugs (SLCD) altogether for 6 days, it yielded even more neurons (Figures 1F–1H). Quantitatively, the neuronal yield (converted neurons/astrocyte number before drug treatment) reached 71% when the four drugs (SLCD) were applied together (Figures S1H and S1I). Therefore, the four drugs together (SLCD) are referred as "core drugs" hereafter, and the core drug-converted neurons are referred to as induced neurons or "iNs" to be consistent with other studies (Yang et al., 2011). It is worth mentioning that the chemically converted iNs and the remaining non-converted astrocytes formed a neuron-astrocyte co-culture condition, with the iNs migrating onto the surface of astrocytes, and the astrocytes served as a feeder layer to promote neuronal survival and maturation (Figure S1J) (Tang et al., 2013).

We then performed a lineage-tracing experiment using GFAP:GFP retroviruses to label HAs with GFP before drug treatment (Figure S2A). The GFP-labeled astrocytes became NeuN+ (RBFOX3) neurons after core drug treatment (Figure S2A, top row), but remained $GFAP^+$ astrocytes in the DMSO control group (Figure S2A, bottom row). To observe the astrocyte-to-neuron conversion process, we performed long-term time-lapse imaging for eight consecutive days on a group of GFP-labeled HAs during and after core drug treatment (Video S1). As shown in the video, the initial flat HAs infected with GFP lentiviruses gradually changed their morphology into neuron-like cells with extended long neurites after core drug treatment (see Video S1 in Supplemental Information). Following time-lapse imaging, we further performed post-fix immunostaining and confirmed that the GFP-labeled neuron-like cells after core drug treatment were indeed immunopositive for NeuN (Figure S2B). Importantly, we did not observe significant cell proliferation during the 8 days of time-lapse imaging (Video S1), consistent with the Ki67 immunostaining results showing an inhibition of cell proliferation by core drug treatment (Figures S2C and S2D, ~130 Ki67+ cells/field before drug treatment and ~10 Ki67+ cells/field after drug treatment). Moreover, NESTIN staining rarely showed neuroprogenitor cells induced by core drugs (Figures S2E and S2F). Together, through lineage tracing, time-lapse imaging, and Ki67 and NESTIN staining, we show that HAs can be directly converted into neurons by four molecules.

Can HAs spontaneously turn into neurons during our experimental process? To test this idea, we performed DCX and TUJ1 (TUBB3) staining but did not observe a significant number of newborn neurons in the DMSO control group from day 2 to day 7 (Figures S3A and S3B, quantified in Figures S3C–S3F). In the core drug-treated group, DCX and TUJ1 signals did not change much at day 2 and day 4, but dramatically increased at day 7 (Figures S3A–S3F), suggesting that it takes ~1 week for HAs to be chemically converted into neurons. At day 14 of the DMSO control group, we did see a few neurons, which were eliminated if the N2 supplement was removed from the culture medium (Figures S3G–S3J), suggesting that the N2 supplement may have a very weak neural induction role in cell cultures.

We further tested whether our core drugs could reprogram different sources of HAs into neurons. After purchasing a different line of HAs from Lonza (cc-2565), we found that our core drugs (4-day treatment of 2.5 μM SB431542, 0.125 μM LDN193189, 0.75 μM CHIR99021, and 2.5 μM DAPT) also induced a large number of iNs (Figures S3K–S3N, immunostained at day 10). Therefore, we conclude that HAs from different sources can be chemically converted into neurons.

Transcriptional Regulation and MECP2-REST Signaling Change during Chemical Reprogramming

What is the molecular mechanism underlying the core drug reprogramming? Our real-time PCR experiments showed that the basic-helix-loop-helix neural transcription

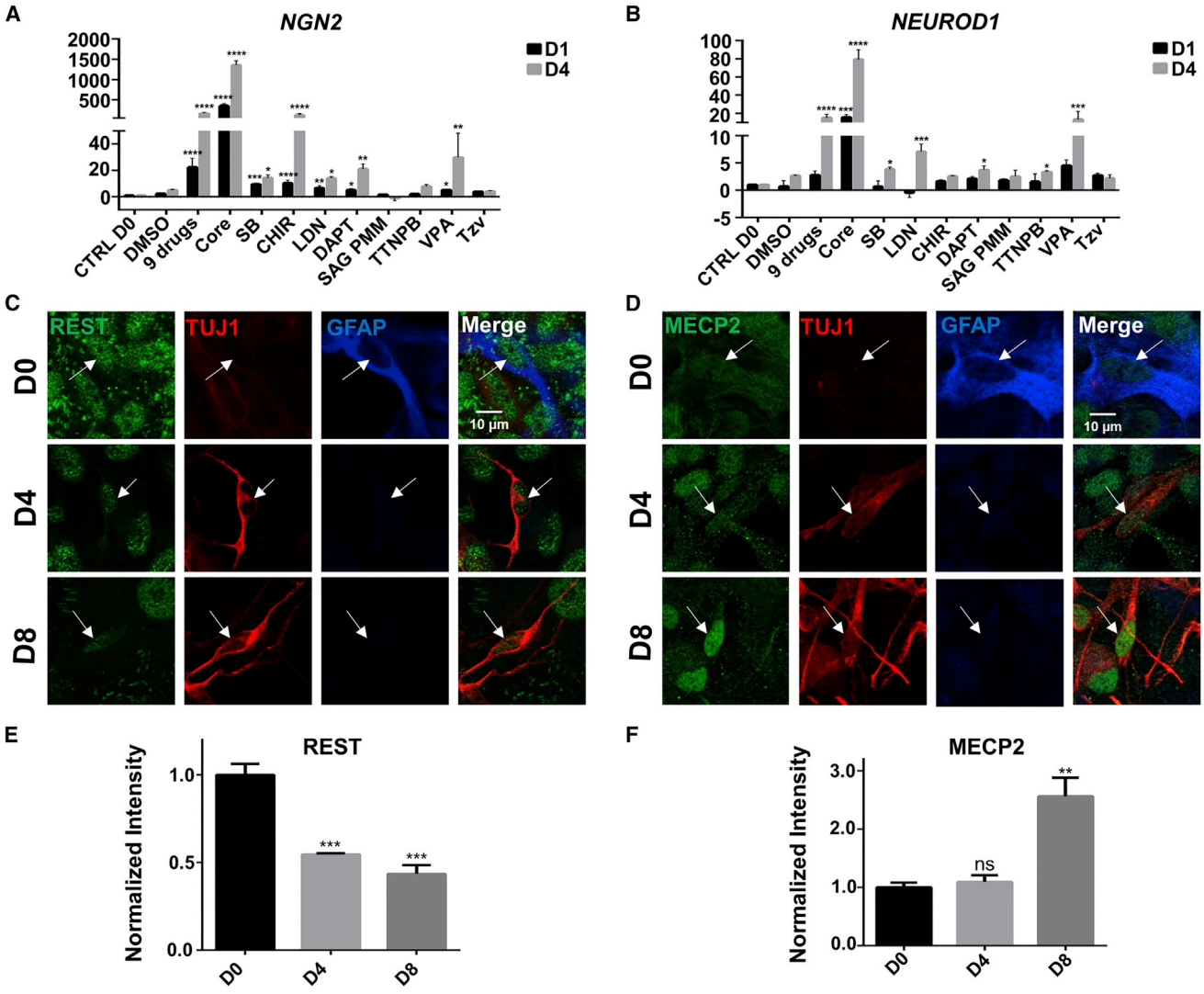

Figure 2. Transcriptional Regulation during Chemical Reprogramming

(A and B) Real-time qPCR analyses revealed transcriptional activation of *NGN2* (A) and *NEUROD1* (B) by core drug treatment. Note than *NGN2* was activated earlier than *NEUROD1*, and that the core drug group showed higher levels of *NGN2* and *NEUROD1* than the nine-drug group. Among individual drugs, SB431542, CHIR99021, LDN193189, DAPT, and VPA increased *NGN2* to a significant level, whereas SB431542, LDN193189, DAPT, TTNPB, and VPA significantly increased the expression of *NEUROD1*. *$p < 0.05$, **$p < 0.01$, ***$p < 0.001$, ****$p < 0.0001$, one-way ANOVA after $\log_2$ transformation, Dunnett's multiple comparison test. Data are represented in means ± SEM. N = 3 batches.

(C and D) Immunostaining showed a gradual decrease of REST (green) during chemical reprogramming of astrocytes (GFAP, blue) into neurons (TUJ1, red) (C). Immunostaining of MECP2 (green) showed a gradual increase during chemical reprogramming (D). Scale bars, 10 μm.

(E and F) Quantified data showing the opposite change of REST and MECP2 during chemical reprogramming. **$p < 0.01$, ***$p < 0.001$, one-way ANOVA followed by Dunnett's multiple comparison test. Data are represented in means ± SEM. N = 3 batches.

factors, including both NEUROD1 and NGN2, were significantly upregulated at day 1 and day 4 by core drug treatment (Figures 2A and 2B), whereas the astrocytic GFAP expression was downregulated (Figure S4A). Interestingly, each individual drug among the four core drugs upregulated *NGN2* level (Figure 2A), and the *NEUROD1* level was upregulated by LDN193189, SB431542, and DAPT (Figure 2B). VPA, an HDAC inhibitor that alters histone acetylation and gene transcription, was found to induce a significant increase of both *NEUROD1* and *NGN2* expression

(Figures 2A and 2B). However, when VPA was added together with the four core drugs, it unexpectedly decreased the reprogramming efficiency (Figures S4B and S4C). We then further tested core drugs in combination with other individual drugs including ROCK inhibitor Tzv, retinoic acid receptor agonist TTNPB, sonic hedgehog activator SAG, and Purmo. Addition of Tzv to the core drugs showed no effect (Figure S4D), while addition of TTNPB decreased the reprogramming efficiency (Figure S4E and quantified in S4G). Addition of SAG and Purmo significantly increased astrocytic proliferation, resulting in overgrown astrocytes and decrease of neurons (data not shown). These results suggest that alteration of extra signaling pathways in addition to the four pathways modulated by core drugs might result in reduced conversion efficiency.

Besides transcriptional regulation of *NGN2* and *NEUROD1*, we further discovered a significant change of REST (RE1-silencing transcription factor) and MECP2 (methyl CpG binding protein 2) signals during core drug-mediated chemical reprogramming (Figures 2C–2F). REST is a transcriptional repressor that can silence neuronal genes in stem cells and non-neuronal cells (Ballas et al., 2005). During neuronal differentiation, REST is downregulated in neurons. We found a significant decrease of REST expression during chemical reprogramming process, particularly in Tuj1$^+$ neurons (Figure 2C, quantified in Figure 2E), indicating the suppression of REST by core drugs during chemical conversion. In contrast, the expression level of MECP2, a nuclear protein that can regulate the expression of many genes including suppressing REST (Skene et al., 2010), increased significantly after core drug treatment (Figure 2D, quantified in Figure 2F). MECP2 has been reported to be highly expressed in neurons, much more than that in astrocytes (Kishi and Macklis, 2004; Skene et al., 2010). Consistently, we found that the increase of MECP2 signal was coinciding with an increase of Tuj1 and a decrease of GFAP signal after core drug treatment. Together, the changes of REST and MECP2 expression level indicate a cell fate change from astrocytes to neurons induced by core drug treatment.

Neuronal Identity after Core Drug Reprogramming

We next characterized the neuronal identity after chemical reprogramming by performing immunostaining on a series of neuronal markers. The core drug-converted human neurons (3 months after drug treatment) were mainly immunopositive for PROX1, CTIP2 (BCL11B), and TBR1 (Figures 3A–3C), but negative for other neuronal markers such as CUX1, NURR1 (NR4A2), and HOXB4 (Figures 3D–3G; quantified in Figure 3H). These results were further confirmed with real-time PCR analysis (Figure 3I). When examining neurotransmitter subtypes, we found that the majority of neurons converted from human cortical astrocytes were immunopositive for VGlut1 (SLC17A7) (78%), a glutamatergic neuron marker, but very few were GABAergic (GAD67 [GAD1], 2%) or dopaminergic neurons (TH, 1%) (Figures 3J–3M). However, when testing our core drug combination in midbrain HAs (ScienCell, 1850), we found a large proportion of converted iNs co-expressing GABA and GAD67 (Figure S5A–S5F), suggesting that different lineages of astrocytes originated from different brain regions may be chemically converted into different subtypes of iNs. Therefore, human cortical astrocytes can be converted into cortical glutamatergic neurons, and different lineages of astrocytes may have their own intrinsic factors to influence the final cell fate after conversion.

Functional Characterization of Core Drug-Converted iNs

We further investigated whether the core drug-converted iNs were functionally connected to each other. Different from mouse neuron cultures, we found that the core drug-converted human neurons could survive for 3–7 months in our cell culture condition and form robust synaptic connections (Figures 4A and 4B). Some core drug-converted human neurons could survive as long as 7.5 months (Figure 4B), providing an extended time window for future studies on drug screening or disease modeling. Functionally, patch-clamp recordings revealed that our chemically converted iNs showed large sodium and potassium currents (Figure 4C) as well as repetitive action potentials (Figure 4F). As expected, converted iNs showed a clear developmental time course of functional maturation when analyzed from 1- to 3-month cultures after chemical conversion. Specifically, sodium currents increased from 1 nA at 1-month culture to 3 nA at 3-month culture, while potassium currents increased from ~2 nA at 1-month culture to ~3.5 nA at 3-month culture (Figures 4D and 4E). The number of cells firing repetitive action potentials increased from 12/35 at 1-month culture to 27/29 at 3-month culture (Figure 4G). The membrane capacitance also increased (Figure S5G, indicating cell growth), together with a decrease of membrane resistance (Figure S5H, an indication of channel and receptor expression) from 1- to 3-month cultures. We also detected glutamate- and GABA-induced receptor currents in 2-month-old converted iNs (Figure 4H), which was consistent with the immunostaining of glutamate receptors (GluR1 and GluR2 subunits) (Figures S5J and S5K) and $GABA_A$ receptors (γ2 and α5 subunits) (Figures S5L and S5M). Moreover, we recorded robust spontaneous synaptic activities, some in burst activity pattern, in 3-month-old cultures after chemical conversion (Figure 4I), suggesting the formation of a highly integrated neural network among the converted iNs. Notably, most of the synaptic events were blocked by

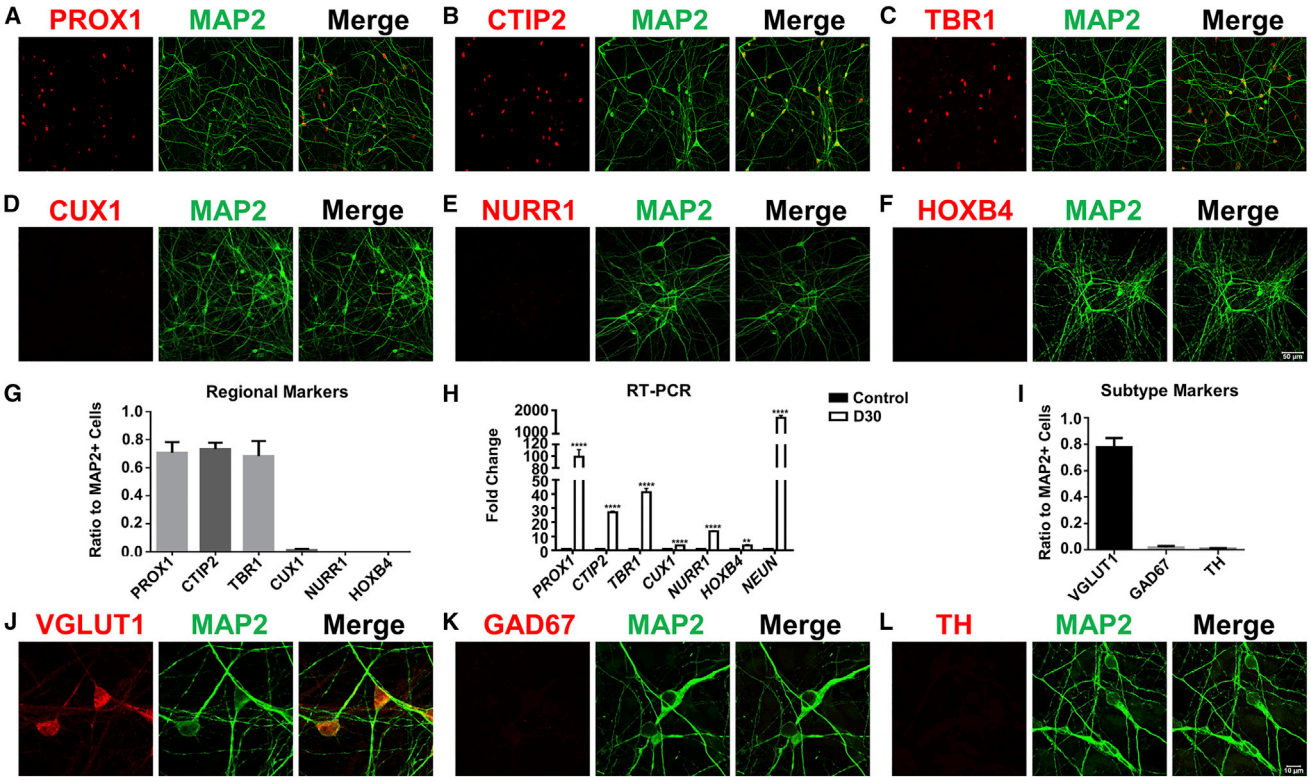

Figure 3. Characterization of Human Neuron Subtypes after Core Drug-Mediated Reprogramming

(A–F) Representative images illustrating the immunostaining of hippocampal neuron marker PROX1 (A, red), forebrain deep layer marker CTIP2 (B, red), cortical neuron marker TBR1 (C, red), cortical superficial layer marker CUX1 (D, red), midbrain marker NURR1 (E, red), hindbrain marker HOXB4 (F, red), and neuronal dendritic marker MAP2 (A–F, green). Scale bar, 50 μm.

(G) MAP2-positive neurons were also immunopositive for PROX1 (71% ± 8%), CTIP2 (73% ± 4%), and TBR1 (68% ± 11%), but not other markers. N ≥ 3 batches.

(H) Real-time PCR experiments were performed at 1 month after core drug treatment to assess different neuronal gene expression level. All data were normalized to human astrocyte control. **p < 0.01, ****p < 0.0001, unpaired t test after $\log_2$ transformation. Data are represented in means ± SEM. N = 3 batches.

(I–L) Immunostaining (I) with different neuronal subtype markers revealed that the human astrocyte-converted iNs (MAP2, green) after core drug treatment were mostly glutamatergic (VGlut1, red) (J), and rarely GABAergic (GAD67, red) (K) or dopaminergic (TH, red) (L). Data are represented in mean ± SEM. N = 3 batches. Scale bar, 10 μm.

glutamate receptor antagonist DNQX (Figure 4I), consistent with their glutamatergic identity shown in Figure 3. Therefore, the four core drugs (SLCD) can chemically reprogram HAs into highly functional neurons.

Signaling Pathways Critical for Chemical Reprogramming

After identifying the four core drugs (SLCD), we further tested whether these particular four drugs were unique for chemical reprogramming, or rather they could be replaced by other functional analogs modulating similar signaling pathways. For example, SB431542 is a TGF-β inhibitor and inhibits a subfamily of activin receptor-like kinase (ALK) receptors including ALK4, ALK5, and ALK7 (Inman et al., 2002). We therefore substituted SB431542 with its functional analogs Repsox (1 μM) or A-8301 (0.25 μM), which also inhibit TGF-β pathway. Interestingly, we found that HAs were also efficiently reprogramed into neurons by substituting SB431542 with Repsox or A-8301 among the four-drug combination (Figures 5A–5C). Thus, inhibiting the TGF-β signaling pathway in general, rather than any particular inhibitor, is critical for chemical reprogramming. Similarly, replacing LDN193189, an inhibitor of BMP through inhibiting another ALK subfamily (ALK2 and ALK3), with other two BMP inhibitors Dorsomorphin (1 μM) or DMH 1 (1.5 μM), also resulted in a significant neuronal reprogramming (Figures 5D–5F). CHIR99021 is a selective inhibitor of GSK-3 and indirectly activates the WNT signaling pathway. CHIR99021 has been used in several studies to generate neurons from ESCs or iPSCs

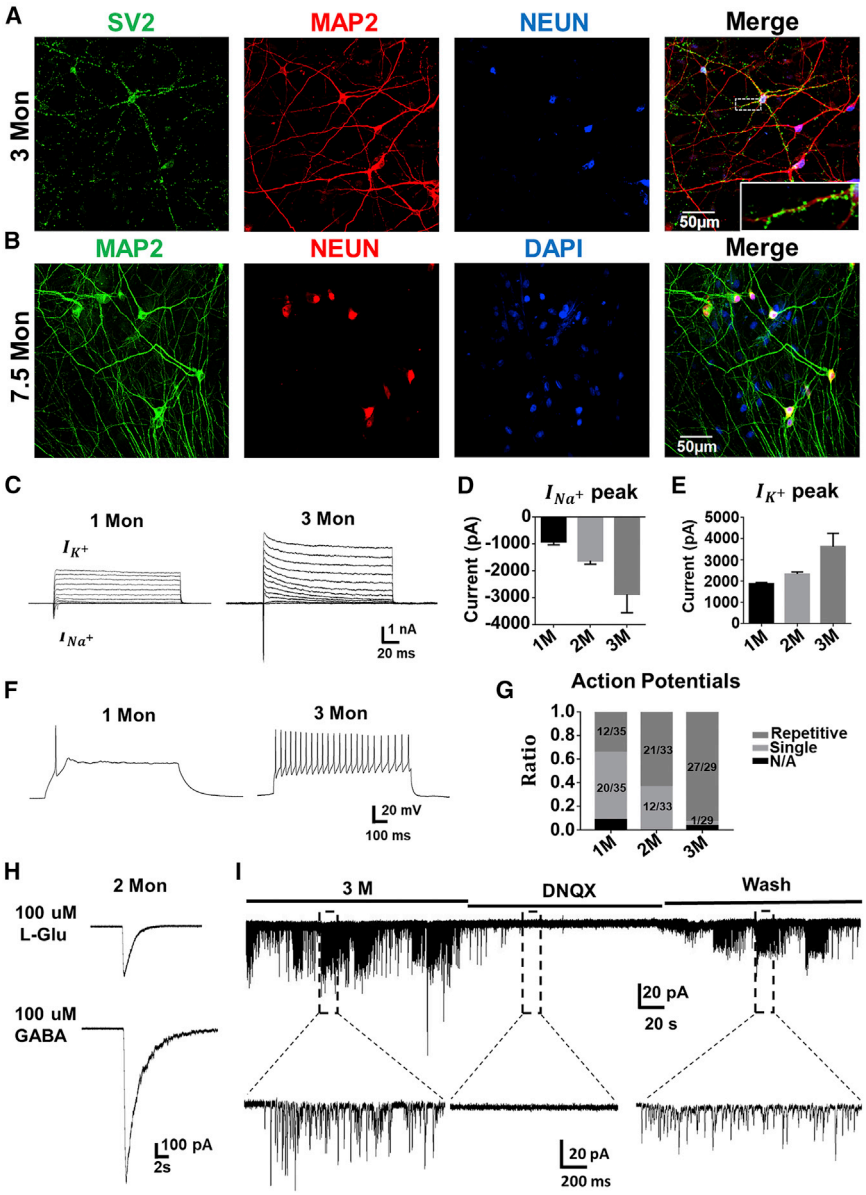

Figure 4. Functional Characterization of the Core Drug-Converted Human Neurons

(A and B) Human astrocyte-converted iNs (MAP2, red; NEUN, blue) induced by core drug treatment showed robust synaptic puncta (SV2, green) after 3 months of culture. N = 3 batches (A). Neurons reprogrammed from HA could survive as long as 7.5 months. N = 3 batches (B). Scale bars, 50 μm.

(C–E) Representative traces of sodium and potassium currents recorded from converted iNs (C), with quantitative analyses showing the developmental increase of peak I_{Na}+ (D) and I_K+ (E).

(F and G) Whole-cell recordings revealed an increase of action potential firing from 1- to 3-month-old cultures after core drug-mediated chemical conversion (F), with quantitative result showing the ratio of converted iNs having repetitive action potential firing at different time points (G).

(H) Representative traces showing glutamate-induced (100 μM) or GABA-induced (100 μM) currents in 2-month-old converted iNs.

(I) Representative trace showing robust synaptic burst activities, which were blocked by glutamate receptor antagonist DNQX, confirming glutamatergic property.

Data are represented as means ± SEM. N ≥ 29.

(Fasano et al., 2010; Kriks et al., 2011), and WNT has been shown to regulate postnatal and adult neurogenesis (Lie et al., 2005; Zhang et al., 2011). Replacement of CHIR99021 by two other GSK-3 inhibitors, SB216763 (1 μM; different from TGF-β inhibitor SB431542) or AR-A014418 (6 μM), resulted in a large number of neurons but less than the effect of CHIR99021 itself (Figures 5G–5I). Lastly, DAPT inhibits Notch signaling pathway by targeting γ-secretase and is involved in the maintenance of the proliferative and undifferentiated state of embryonic stem cells during development (Urban and Guillemot, 2014). Replacing DAPT with other two Notch inhibitors, BMS906024 (2 μM) or RO4929097 (0.5 μM), resulted in comparable reprogramming efficiency (Figures 5J–5L), suggesting an important role of Notch signaling in neuronal conversion. After testing each individual signaling pathway with at least three different inhibitors, we replaced all of the original four core drugs (SLCD) with their functional analogs, Repsox, Dorsomorphin, SB216763, and RO4929097 (RDSRo). The four functional analogs (RDSRo) together also generated a large number of converted iNs, with the conversion efficiency reaching ~70% of the original core drug group (Figures 5M–5O). Similar to the core drug group (SLCD), the RDSRo group also induced mainly glutamatergic neurons but not GABAergic or dopaminergic neurons (Figures S6A–S6C)

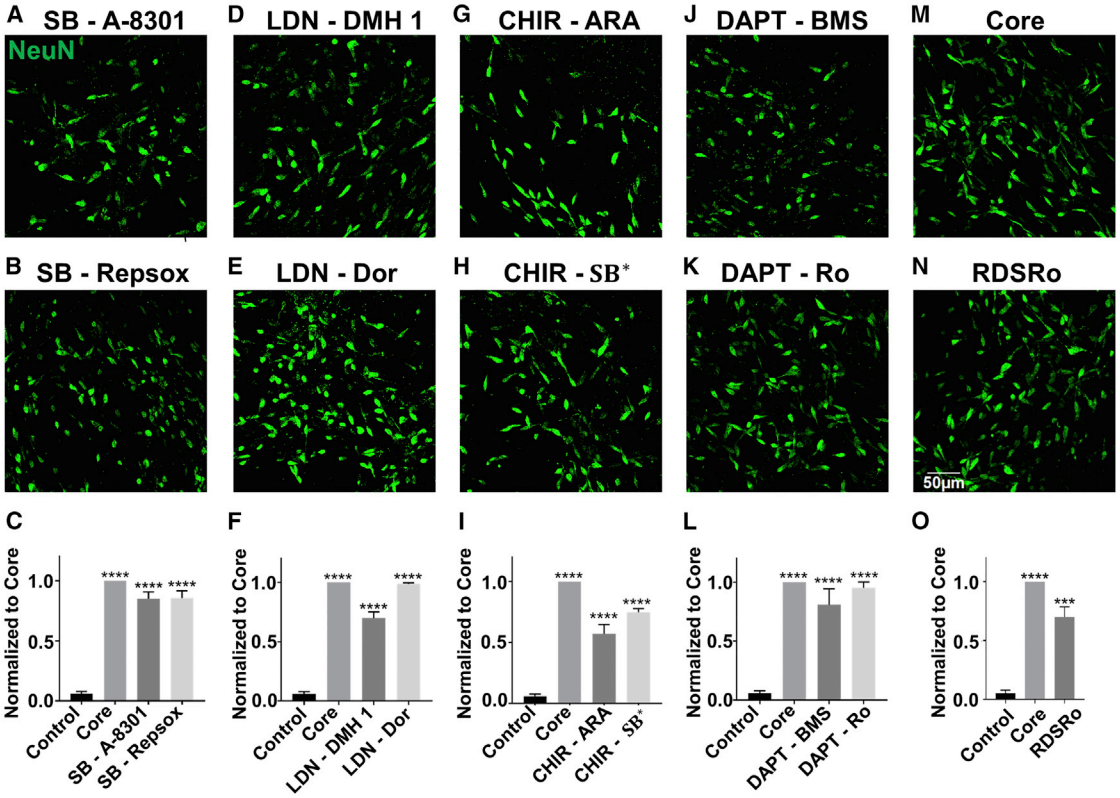

Figure 5. Drug Replacement Revealed Key Signaling Pathways Involved in Chemical Reprogramming

(A–C) Among core drugs, replacing SB431542 with its functional analog A-8301 (A) or Repsox (B) yielded similar numbers of reprogrammed neurons (87% ± 4% for A-8301 and 89% ± 6% for Repsox replacement group) (C). Immunostaining of NEUN was performed 14 days after the start of drug treatment.

(D–F) Replacing LDN193189 with its functional analog DMH 1 (D) or Dorsomorphin (E) resulted in similar conversion efficiency (70% ± 5% for DMH 1 and 97% ± 1% for Dorsomorphin) (F).

(G–I) Replacing CHIR99021 with its functional analog ARA014418 (G) or SB216763 (H) yielded less numbers of neurons (57% ± 4% for ARA014418 and 76% ± 3% for SB216763) (I).

(J–L) Replacing DAPT with its functional analog BMS906024 (J) or RO4929097 (K) also achieved similar conversion efficiency (81% ± 1% for BMS906024 and 95% ± 5% for RO4929097) (L).

(M–O) Replacing the four core drugs (M) with their corresponding functional analogs RDSRo (N, SB431542 replaced by Repsox, LDN193189 by Dorsomorphin, CHIR99021 by SB216763, and DAPT by RO4929097) resulted in lower reprogramming efficiency (66% ± 16%) (O).

***p < 0.001, ****p < 0.0001, one-way ANOVA followed with Dunnett's multiple comparison test. Data are represented in means ± SEM. N = 3 batches. Scale bar, 50 μm.

and formed local synaptic connections (Figure S6D). Consistently, real-time PCR analysis revealed that both core drug group or their various substitution groups all downregulated glial genes such as *Glt1* (*SLC1A2*) (Figures S6E and S6F). Furthermore, real-time PCR experiments identified significant changes of gene targets that are correlated with the four signaling pathways, including *NEUROGENIN 1* for the GSK-3β pathway (Hirabayashi et al., 2004), *UNC13A* for the Notch pathway (Li et al., 2012), *ID1* for the BMP pathway (Morikawa et al., 2011), and *COL1A1* for the TGF-β pathway (Verrecchia et al., 2001) (Figure S6G). Altogether, these results suggest that modulation of four signaling pathways including TGF-β, BMP, GSK-3, and Notch in HAs is sufficient for reprogramming into functional neurons.

Further Down-Selection of Small Molecules for Chemical Reprogramming

To investigate whether the four-drug cocktail (SLCD) is the minimal combination capable of reprogramming HAs into neurons, we further tested all possible combinations of three drugs, two drugs, and each individual drug, among the four-drug cocktail (SLCD). Interestingly, all three-drug combinations were capable of reprogramming HAs into

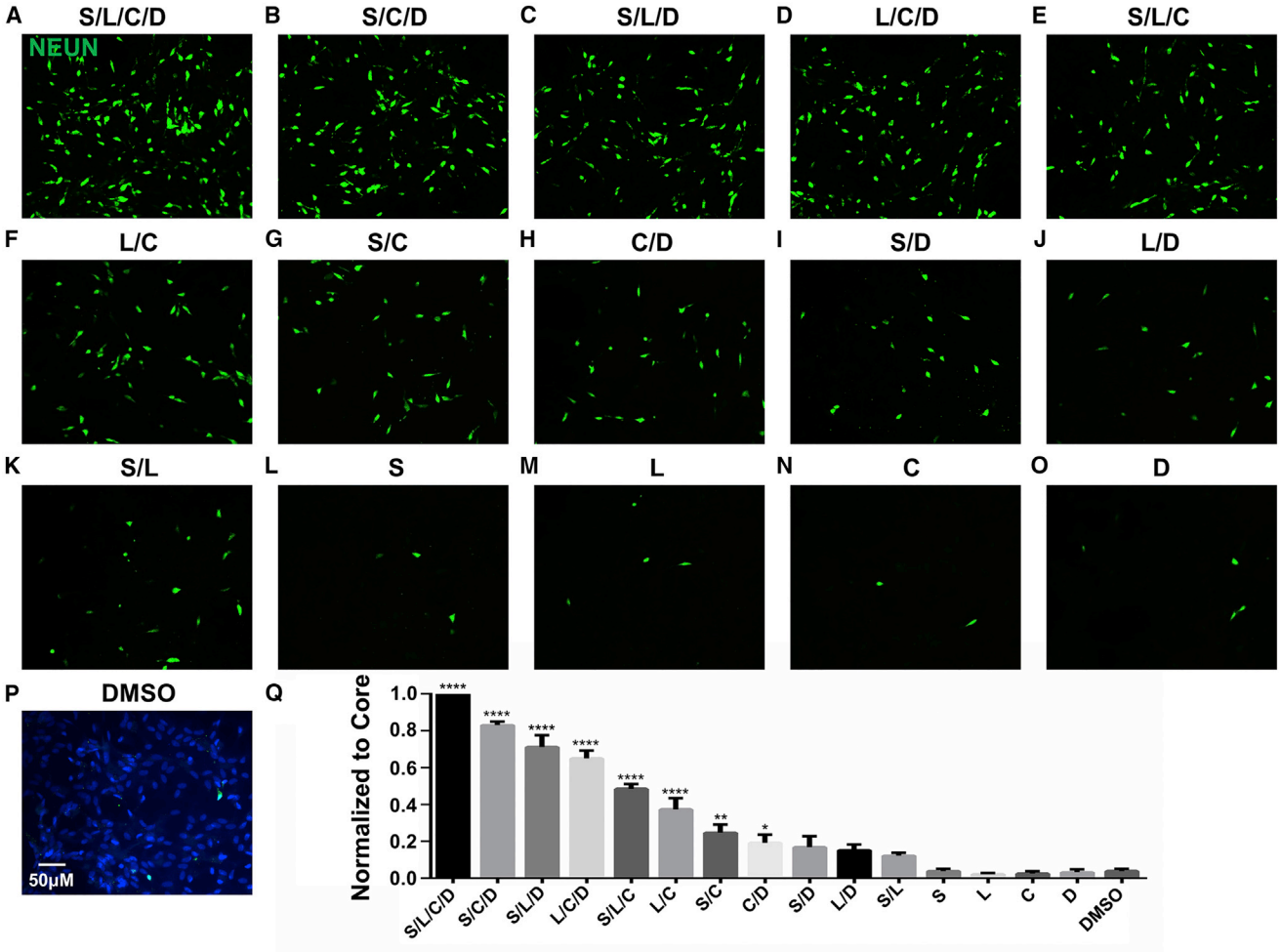

Figure 6. A Systematic Investigation of Chemical Reprogramming Efficiency among Various Combinations of Fewer Core Drugs

(A) Core drug (S for SB431542, L for LDN193189, C for CHIR99021, or D for DAPT)-induced chemical reprogramming of HA into neurons (NEUN, green) as a control. For all experiments in this figure, immunostaining was performed at 14 days after initial drug treatment.

(B–E) Three-drug combinations, including S/C/D (B), S/L/D (C), L/C/D (D), and S/L/C (E), among the four core drugs could also reprogram a significant number of HAs into neurons, although with lower efficiency compared with the four core drugs.

(F–K) Two-drug combinations, including L/C (F), S/C (G), C/D (H), S/D (I), L/D (J), and S/L (K), also induced some neurons, especially those combinations containing CHIR99021 (F–H).

(L–P) Few neurons were found when treated with each individual drug, including S (L), L (M), C (N), and D (O), compared with the DMSO control (P). Scale bar, 50 μm in (A–P).

(Q) Quantification of all combinations among the four core drugs. *$p < 0.05$, **$p < 0.01$, ****$p < 0.0001$, one-way ANOVA followed with Dunnett's multiple comparison test. Data are represented in means ± SEM. N = 3 batches.

neurons but with lower efficiency compared with the four-drug group (Figures 6A–6E). Notably, the combination of three drugs SB431542/CHIR99021/DAPT reached >80% of the four-drug efficiency (Figure 6Q, One-way ANOVA followed with *post hoc* Dunnett's multiple comparison test, $n \geq 3$ batches). On the other hand, all combinations of two drugs showed significantly diminished reprogramming efficiency, with the highest one (LDN193189/CHIR99021) still <40% of that induced by the four-drug cocktail (Figures 6F–6K, quantified in Figure 6Q). None of the individual drugs among the four core drugs showed any significant difference from the DMSO control (Figure 6L–6P, quantified in Figure 6Q). real-time PCR analysis also showed that the core drugs and combinations of three or two drugs all downregulated astrocytic genes such as *S100β* and *Glast* (*SLC1A3*) (Figures S6H–S6I). These studies demonstrate that HAs may be chemically reprogrammed into neurons by simultaneously modulating at least three

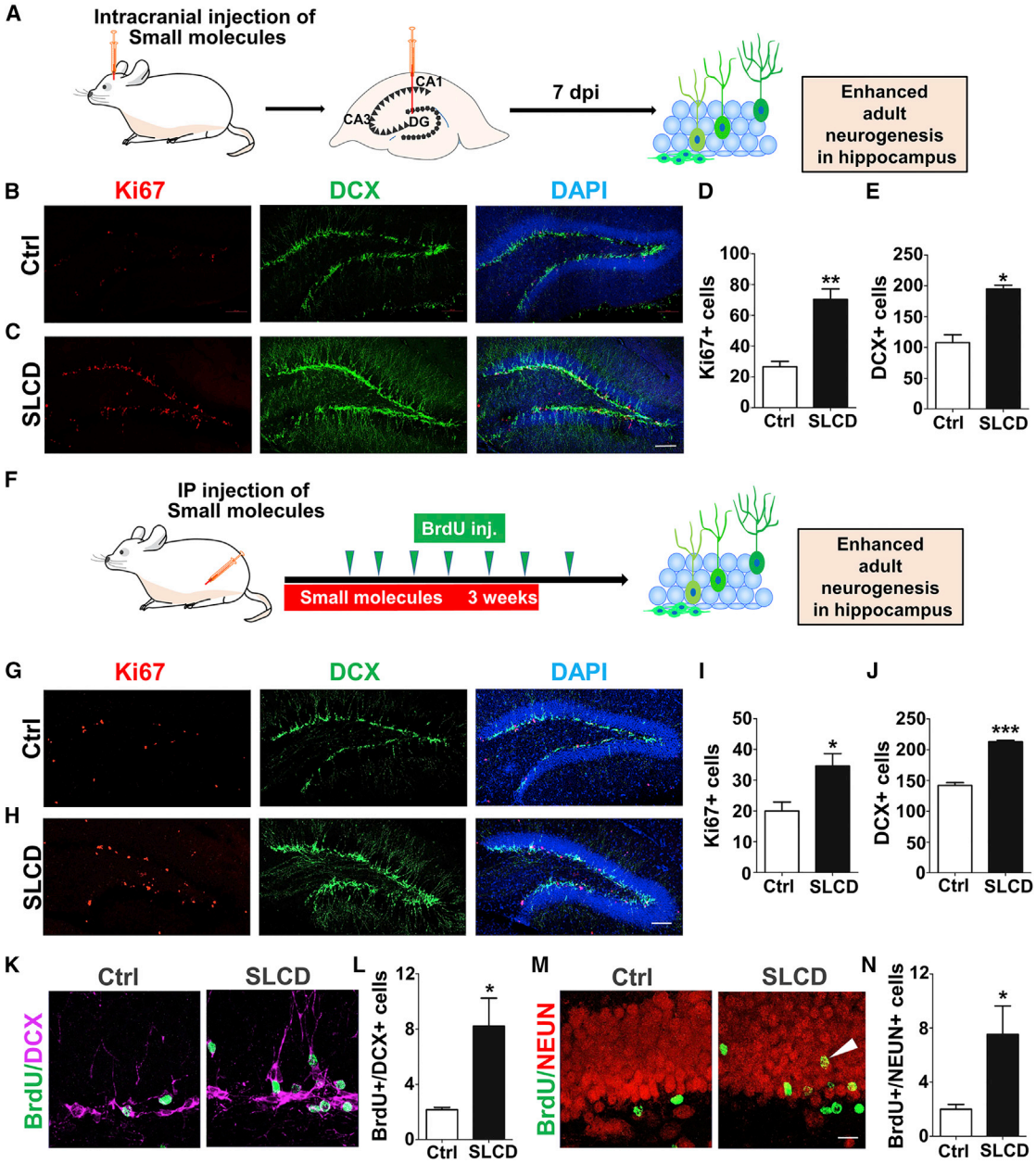

Figure 7. Significant Increase of Adult Neurogenesis after *In Vivo* Application of Core Drugs

(A) Schematic drawing illustrating a single dose of core drug injection into the dentate gyrus of mouse brains. After 7 days, the mice were sacrificed for immunostaining.

(B–E) Representative images (B and C) and quantitative analyses (D and E) showing that core drugs significantly increased the number of dividing cells (Ki67, red) and newborn neurons (DCX, green). Student's t test, *$p < 0.01$, **$p < 0.001$, $N = 4$ mice. Scale bar, 100 μm.

(F) Schematic drawing illustrating intraperitoneal injection of core drugs (SB 431542, 165 μM; LDN193189, 8.25 μM; CHIR99021, 49.5 μM; and DAPT, 165 μM; all in 20% captisol, 10 mL/kg) daily for 23 days. BrdU was administrated every 3–4 days from day 5 to day 26. The mice were sacrificed at day 32 for immunostaining.

(G–J) Representative images (G and H) and quantitative analyses (I and J) showing that core drugs significantly increased the cell number of dividing cells (Ki67, red) and newborn neurons (DCX, green) compared with vehicle control with 20% captisol (CPTS) injection (Student's t test, *$p < 0.01$, ***$p < 0.0001$, $N = 4$ mice). Scale bar, 100 μm. The total cell number of Ki67+ or DCX+ cells in one side of the dentate gyrus was quantified based on 10 stacked images with a total thickness of 18 μm and a volume of ~0.014 mm^3.

(legend continued on next page)

or two signaling pathways, but not by changing a single signaling pathway.

Regulation of Adult Neurogenesis through *In Vivo* Administration of Small Molecules

With successful conversion of cultured HAs into neurons *in vitro*, we then injected the core drugs into mouse brains to test whether they can convert astrocytes into neurons *in vivo*. After spending several years using various methods to deliver small molecules in the mouse brain *in vivo*, we have not achieved definitive success of chemical conversion inside mouse brains despite the observation of a few neurons after chemical treatment. This is rather disappointing, but we are still continuously trying direct *in vivo* chemical conversion in the mouse brain. The biggest challenge for *in vivo* chemical conversion is how to maintain a constant concentration of small molecules inside the brain without causing a severe invasive damage to the brain. We have tried using biomaterial to encapsulate small molecules, but, perhaps because our small molecules are too small or we have not found the right biomaterial for such small molecules, the small molecules we applied might not stay for a long time inside the brain. We also tried an osmotic minipump (Alzet) but the tip of the insertion caused significant tissue damage inside the brain, and the injury induced many DCX+ cells that were mainly reactive astrocytes 2 weeks after drug treatment (Figures S7I–S7K). On the other hand, during our vigorous testing of *in vivo* chemical reprogramming, we accidentally found that core drugs significantly increased adult neurogenesis in the mouse hippocampus (Figure 7). We initially injected core drugs through intracranial injection into the hippocampus and sacrificed the mice 7 days later (Figure 7A). We observed remarkable increase of DCX-labeled newborn neurons together with Ki67-labeled proliferative cells in the dentate granule layer (Figures 7B–7E). When separating the four core drugs into two-drug combinations (CHIR99021 + DAPT; and SB431542 + LDN193189), we found that the two-drug combinations could also increase adult hippocampal neurogenesis (Figures S7A–S7H). However, the four drugs together were more potent in promoting neuronal maturation, as shown by more complex dendritic morphology and more neurons migrated into the outer granule layer (Figures S7A–S7H).

We next further tested whether our core drugs can pass through blood-brain barrier (BBB) to regulate adult neurogenesis through intraperitoneal (i.p.) administration (daily i.p. injection of core drugs for 3 weeks, and bromodeoxyuridine (BrdU) was i.p. injected every 3–4 days from day 5 to day 26 to identify newborn cells) (Figure 7F). It is important to note that the intracranial injection of core drugs was one-time injection, whereas the i.p. injection was repeat injections over 3 weeks. Interestingly, i.p. injection of core drugs also resulted in a significant increase of DCX-labeled newborn neurons and Ki67-positive cells in the dentate granule layer (Figures 7G–7J). Moreover, BrdU-labeled cells that were dually immunopositive for DCX or NEUN increased significantly after i.p. injection of core drugs (Figures 7K–7N), with more newborn neurons migrating toward the outer layer of the dentate granule layer than in control group (Figure 7M, arrowhead), suggesting an accelerated neuronal maturation after core drug treatment. These results suggest that core drugs can regulate adult neurogenesis *in vivo*.

DISCUSSION

In this work, we identified a chemical formula using only three to four small molecules to reprogram HAs into neurons. Through replacement of different functional analogs, we demonstrate that modulating multiple signaling pathways, but not a single signaling pathway, is important for chemical reprogramming of astrocytes into neurons. The chemically converted iNs can survive more than 7 months and are highly functional with bursts of synaptic activities. Besides upregulation of neural transcription factors such as *NEUROD1* and *NGN2*, we found that the neural suppressor gene REST was significantly downregulated, while MECP2 was upregulated during chemical conversion. During our attempt to chemically convert astrocytes into neurons in the mouse brain *in vivo*, we accidentally discovered that our core drugs can potently regulate adult neurogenesis in the mouse hippocampus. Together, our chemical formula with only three to four small molecules to reprogram HAs into neurons brings us one step closer toward a potential drug therapy for brain repair.

One discovery made in this study is the synergistic modulation of multiple signaling pathways that are critical for chemical reprogramming. Modulating a single signaling pathway alone is not sufficient to change the cell fate. For example, while CHIR99021 alone increased *NGN2* by 120-fold, it did not convert astrocytes into neurons, suggesting that modulating a single signaling pathway is not sufficient

(K and L) Representative images (K) and quantitative analysis (L) showing the number of cells colabeled by BrdU (green) and DCX (magenta) was enhanced by core drug treatment (Student's t test, *$p < 0.01$, N = 4 mice).
(M and N) Representative images (M) and quantitative analysis (N) showing the number of cells colabeled by BrdU (green) and NEUN (red) was increased in granular layer by core drugs (Student's t test, *$p < 0.01$, N = 4 mice). Scale bar, 20 μm.

for chemical conversion. Nevertheless, CHIR99021 is one of the most widely used small molecules in chemical reprogramming studies (Hu et al., 2015; Li et al., 2015; Zhang et al., 2015). Application of SB431542 and LDN193189 together has been reported to induce neurogenesis from stem cells (Chambers et al., 2009), but they are not sufficient to reprogram HAs into neurons, suggesting that HAs, as terminally differentiated cells, are very different from neural stem cells in terms of reprogrammability. By substituting each core drug with its functional analogs, we further demonstrate that it is not the specific drugs (SLCD) per se but rather the four signaling pathways (Notch, GSK-3β, TGF-β, and BMP) that are regulated by the four core drugs are critical for chemical reprogramming. Interestingly, modulating any three out of the four signaling pathways can successfully reprogram HAs into neurons, suggesting that these four pathways may have some overlapping functions. It is worth mentioning that, during the progress of this study, Dr. Pei's group reported that human adult astrocytes isolated from patients with brain tumor can be reprogrammed into neurons by a six-small-molecule cocktail VCRFBI (VPA, CHIR99021, Repsox, forskolin, i-Bet151, and ISX-9) (Gao et al., 2017). This is a very interesting work because it represents another major step toward a future clinical application to directly convert adult HAs into neurons using a drug approach. On the other hand, it should be cautioned that any astrocytes isolated from the brain and put into Petri dishes may lose their *in vivo* identity. Therefore, it is still pivotal to test whether small molecules can convert HAs directly in a brain circuit *in vivo*. Interestingly, we have unexpectedly found that *in vivo* injection of the core drugs can significantly increase adult neurogenesis in the mouse hippocampus. This finding of small molecules passing through the BBB and regulating adult neurogenesis may have important implications for future development of drug therapies.

Another discovery of this study is that, regardless of nine- or four-molecule cocktails, a common outcome of our chemical reprogramming protocols is the upregulation of neural transcription factors *NEUROD1* and *NGN2*. Consistent with our discovery, recent work on chemical reprogramming of cultured fibroblasts or astrocytes into neurons also reported an upregulation of *NEUROD1* and *NGN2* together with other transcription factors (Cheng et al., 2015; Gao et al., 2017; Li et al., 2015). Therefore, it seems that our chemical reprogramming approach is an upstream process that may trigger the upregulation of neural transcription factors, which then carry on the reprogramming process. Furthermore, we and other groups have reported that overexpression of neural transcription factors NEUROD1 (Guo et al., 2014) and NGN2 (Heinrich et al., 2010) can both convert astrocytes into glutamatergic neurons. Interestingly, both our nine- and four-molecule cocktails convert HAs mainly into glutamatergic neurons as well (Zhang et al., 2015), possibly through the upregulation of *NEUROD1* and *NGN2*. Dr. Pei's group recently also reported that a six-drug cocktail (VCRFBI) converted adult HAs into glutamatergic neurons associated with upregulation of neural transcription factors including *NEUROD1* and *NGN2* (Gao et al., 2017). Notably, our nine-drug cocktail generated a small percentage of GABAergic neurons but a four-drug cocktail did not, suggesting that the small molecules removed in this current study (TTNPB, SAG/Purmo, VPA, TZV) might be responsible for the small number of GABAergic neurons. Further work is needed to find various chemical cocktails that can reprogram HAs into other neuronal subtypes such as GABAergic and dopaminergic neurons. In addition, besides the four signaling pathways identified in this study, other signaling pathways that may also be important for chemical reprogramming of astrocytes into neurons, or to reprogram other glial cells such as NG2 glia into neurons, should be investigated.

In summary, this study reveals a drug formula that uses only three or four small molecules to efficiently reprogram HAs into functional neurons. Such a simple chemical reprogramming protocol makes it possible to develop a potentially useful drug therapy for neuroregeneration and brain repair, although great challenges such as chemical toxicity and CNS drug delivery are yet to be solved in future studies.

EXPERIMENTAL PROCEDURES

Cell Culture

Human cortical astrocytes purchased from ScienCell (1800, San Diego, CA) and Lonza (cc-2565) were subcultured as described previously (Guo et al., 2014; Zhang et al., 2015). In brief, HAs were cultured in a medium (HA medium) containing DMEM/F12 (Gibco), 10% FBS (Gibco), B27 supplements (Gibco), 3.5 mM Glucose (Sigma), 10 ng/mL fibroblast growth factor 2 (FGF2) (Alomone Labs), 10 ng/mL epidermal growth factor (Alomone Labs), and penicillin/streptomycin (Gibco). The human cortical astrocytes used in this study were subjected to 10–15 passages after purchasing from ScienCell, and 6–10 passages after purchasing from Lonza.

To examine whether HAs (ScienCell, 1800) contain any neural progenitor cells (NPCs), we cultured the cells in neuronal differentiation medium for 1 month and then performed immunostaining on different cell markers. As a positive control, human NPCs (gift from Dr. Fred Gage) were cultured on the coverslips coated with 1% Matrigel (Gibco), in NPC proliferation medium containing DMEM/F12, penicillin/streptomycin, B27 supplement, N2 supplement, and FGF2 (20 ng/mL).

Reprogramming HAs to Neurons

HAs were seeded onto coverslips (12 mm) pre-coated with poly-D-lysine (Sigma) in 24-well plates (BD Biosciences) and cultured in HA medium until reaching ~90% confluence. One day before

reprogramming, half of the HA medium was changed to N2 medium, which contained DMEM/F12, N2 supplements (Gibco), and penicillin/streptomycin. The following day, the culture medium would be totally changed to N2 medium, together with small molecules or vehicle control (0.2% DMSO). The culture medium and drugs were refreshed three times every 2 days. In the core drug together group, SB431542, LDN193189, CHIR99021, and DAPT were always applied together to HAs. In the core drug sequential group, SB431542 and LDN193189 were added for 2 days, and then replaced by CHIR99021 and DAPT for another 4 days. In both groups, at 6 days after drug treatment, the culture medium was changed to neuronal differentiation medium consisting of DMEM/F12, N2, B27, 0.5% FBS, 1 μM Y-27632 (Tocris), 5 μg/mL vitamin C, and penicillin/streptomycin (Gibco). To promote long-term neuronal maturation, brain-derived neurotrophic factor (BDNF) (10 ng/mL, Invitrogen), neurotrophin-3 (NT3) (10 ng/mL, Invitrogen) and insulin growth factor 1 (IGF-1) (20 ng/mL, Invitrogen) were added into the neuronal differentiation medium. Importantly, 200 μL medium with BDNF, NT3, and IGF-1 was added to each well every week to prevent the osmolarity change caused by medium evaporation and to keep the total medium volume around 2 mL in 24-well plates.

Statistical Analysis

Data were analyzed using Student's t test for two-group comparison, and one-way ANOVA for multiple-group comparison followed by Dunnett's *post hoc* test in GraphPad. Dunnett's *post hoc* was chosen here because of its power in comparing every mean with a control mean. All data are represented as means ± SEM. *$p < 0.05$, **$p < 0.01$, ***$p < 0.001$, ****$p < 0.0001$.

ACCESSION NUMBERS

Our own RNA-seq data on human fetal astrocytes are available at the GEO (GEO: GSE123397).

Previous datasets published by other labs (Modrek et al., 2017; Zhang et al., 2016b) and used for comparison here are: hNSCs (GSE94962) and human fetal and adult astrocytes (GSE73721).

More Supplemental Experimental Procedures can be found in the Supplemental Information.

SUPPLEMENTAL INFORMATION

Supplemental Information includes Supplemental Experimental Procedures, seven figures, two tables and one video and can be found with this article online at https://doi.org/10.1016/j.stemcr.2019.01.003.

AUTHOR CONTRIBUTIONS

G.C. conceived and supervised the entire project, analyzed the data, and wrote the manuscript. J.-C.Y. performed the majority of the experiments, analyzed the data, and participated in writing the manuscript. L.Z. performed the experiments on MECP2 and REST, and, together with Y.W., X.-Y.H., and Z.-F.L., did *in vivo* work. N.-X.M., G.L., and F.-P.D. performed real-time PCR experiments on regional markers, transcriptional regulation, and pathway targets during chemical reprogramming. G.-Y.W. participated in the discussion and designing of some of the experiments.

ACKNOWLEDGMENT

This work was supported by grants from NIH (AG045656) and Alzheimer's Association (ZEN-15-321972), as well as Charles H. "Skip" Smith Endowment Fund at Pennsylvania State University to G.C. G.C. is a co-founder of NeuExcell Therapeutics.

Received: January 17, 2018
Revised: December 28, 2018
Accepted: January 6, 2019
Published: February 7, 2019

REFERENCES

Ballas, N., Grunseich, C., Lu, D.D., Speh, J.C., and Mandel, G. (2005). REST and its corepressors mediate plasticity of neuronal gene chromatin throughout neurogenesis. Cell *121*, 645–657.

Berninger, B., Costa, M.R., Koch, U., Schroeder, T., Sutor, B., Grothe, B., and Gotz, M. (2007). Functional properties of neurons derived from in vitro reprogrammed postnatal astroglia. J. Neurosci. *27*, 8654–8664.

Burda, J.E., and Sofroniew, M.V. (2014). Reactive gliosis and the multicellular response to CNS damage and disease. Neuron *81*, 229–248.

Cao, N., Huang, Y., Zheng, J.S., Spencer, C.I., Zhang, Y., Fu, J.D., Nie, B.M., Xie, M., Zhang, M.L., Wang, H.X., et al. (2016). Conversion of human fibroblasts into functional cardiomyocytes by small molecules. Science *352*, 1216–1220.

Chambers, S.M., Fasano, C.A., Papapetrou, E.P., Tomishima, M., Sadelain, M., and Studer, L. (2009). Highly efficient neural conversion of human ES and iPS cells by dual inhibition of SMAD signaling. Nat. Biotechnol. *27*, 275–280.

Cheng, L., Gao, L., Guan, W., Mao, J., Hu, W., Qiu, B., Zhao, J., Yu, Y., and Pei, G. (2015). Direct conversion of astrocytes into neuronal cells by drug cocktail. Cell Res. *25*, 1269–1272.

Cheng, L., Hu, W.X., Qiu, B.L., Zhao, J., Yu, Y.C., Guan, W.Q., Wang, M., Yang, W.Z., and Pei, G. (2014). Generation of neural progenitor cells by chemical cocktails and hypoxia. Cell Res. *24*, 665–679.

Fasano, C.A., Chambers, S.M., Lee, G., Tomishima, M.J., and Studer, L. (2010). Efficient derivation of functional floor plate tissue from human embryonic stem cells. Cell Stem Cell *6*, 336–347.

Filous, A.R., and Silver, J. (2016). Targeting astrocytes in CNS injury and disease: a translational research approach. Prog. Neurobiol. *144*, 173–187.

Gao, L., Guan, W., Wang, M., Wang, H., Yu, J., Liu, Q., Qiu, B., Yu, Y., Ping, Y., Bian, X., et al. (2017). Direct generation of human neuronal cells from adult astrocytes by small molecules. Stem Cell Reports *8*, 538–547.

Grande, A., Sumiyoshi, K., Lopez-Juarez, A., Howard, J., Sakthivel, B., Aronow, B., Campbell, K., and Nakafuku, M. (2013). Environmental impact on direct neuronal reprogramming in vivo in the adult brain. Nat. Commun. *4*, 2373.

Guo, Z.Y., Zhang, L., Wu, Z., Chen, Y.C., Wang, F., and Chen, G. (2014). In vivo direct reprogramming of reactive glial cells into functional neurons after brain injury and in an Alzheimer's disease model. Cell Stem Cell *14*, 188–202.

Heinrich, C., Blum, R., Gascon, S., Masserdotti, G., Tripathi, P., Sanchez, R., Tiedt, S., Schroeder, T., Gotz, M., and Berninger, B. (2010). Directing astroglia from the cerebral cortex into subtype specific functional neurons. PLoS Biol. *8*, e1000373.

Hirabayashi, Y., Itoh, Y., Tabata, H., Nakajima, K., Akiyama, T., Masuyama, N., and Gotoh, Y. (2004). The Wnt/beta-catenin pathway directs neuronal differentiation of cortical neural precursor cells. Development *131*, 2791–2801.

Hu, W.X., Qiu, B.L., Guan, W.Q., Wang, Q.Y., Wang, M., Li, W., Gao, L.F., Shen, L., Huang, Y., Xie, G.C., et al. (2015). Direct conversion of normal and Alzheimer's disease human fibroblasts into neuronal cells by small molecules. Cell Stem Cell *17*, 204–212.

Inman, G.J., Nicolas, F.J., Callahan, J.F., Harling, J.D., Gaster, L.M., Reith, A.D., Laping, N.J., and Hill, C.S. (2002). SB-431542 is a potent and specific inhibitor of transforming growth factor-beta superfamily type I activin receptor-like kinase (ALK) receptors ALK4, ALK5, and ALK7. Mol. Pharmacol. *62*, 65–74.

Kishi, N., and Macklis, J.D. (2004). MECP2 is progressively expressed in post-migratory neurons and is involved in neuronal maturation rather than cell fate decisions. Mol. Cell. Neurosci. *27*, 306–321.

Kriks, S., Shim, J.W., Piao, J., Ganat, Y.M., Wakeman, D.R., Xie, Z., Carrillo-Reid, L., Auyeung, G., Antonacci, C., Buch, A., et al. (2011). Dopamine neurons derived from human ES cells efficiently engraft in animal models of Parkinson's disease. Nature *480*, 547–551.

Li, H., and Chen, G. (2016). In vivo reprogramming for CNS repair: regenerating neurons from endogenous glial cells. Neuron *91*, 728–738.

Li, X., Zuo, X.H., Jing, J.Z., Ma, Y.T., Wang, J.M., Liu, D.F., Zhu, J.L., Du, X.M., Xiong, L., Du, Y.Y., et al. (2015). Small-molecule-driven direct reprogramming of mouse fibroblasts into functional neurons. Cell Stem Cell *17*, 195–203.

Li, Y., Hibbs, M.A., Gard, A.L., Shylo, N.A., and Yun, K. (2012). Genome-wide analysis of N1ICD/RBPJ targets in vivo reveals direct transcriptional regulation of Wnt, SHH, and hippo pathway effectors by Notch1. Stem Cells *30*, 741–752.

Lie, D.C., Colamarino, S.A., Song, H.J., Desire, L., Mira, H., Consiglio, A., Lein, E.S., Jessberger, S., Lansford, H., Dearie, A.R., and Gage, F.H. (2005). Wnt signalling regulates adult hippocampal neurogenesis. Nature *437*, 1370–1375.

Liu, Y.G., Miao, Q.L., Yuan, J.C., Han, S.E., Zhang, P.P., Li, S.L., Rao, Z.P., Zhao, W.L., Ye, Q., Geng, J.L., et al. (2015). Ascl1 converts dorsal midbrain astrocytes into functional neurons in vivo. J. Neurosci. *35*, 9336–9355.

Modrek, A.S., Golub, D., Khan, T., Bready, D., Prado, J., Bowman, C., Deng, J.J., Zhang, G.A., Rocha, P.P., Raviram, R., et al. (2017). Low-grade astrocytoma mutations in IDH1, P53, and ATRX cooperate to block differentiation of human neural stem cells via repression of SOX2. Cell Rep. *21*, 1267–1280.

Morikawa, M., Koinuma, D., Tsutsumi, S., Vasilaki, E., Kanki, Y., Heldin, C.H., Aburatani, H., and Miyazono, K. (2011). ChIP-seq reveals cell type-specific binding patterns of BMP-specific Smads and a novel binding motif. Nucleic Acids Res. *39*, 8712–8727.

Niu, W., Zang, T., Zou, Y., Fang, S., Smith, D.K., Bachoo, R., and Zhang, C.L. (2013). In vivo reprogramming of astrocytes to neuroblasts in the adult brain. Nat. Cell Biol. *15*, 1164–1175.

Pekny, M., and Nilsson, M. (2005). Astrocyte activation and reactive gliosis. Glia *50*, 427–434.

Skene, P.J., Illingworth, R.S., Webb, S., Kerr, A.R., James, K.D., Turner, D.J., Andrews, R., and Bird, A.P. (2010). Neuronal MeCP2 is expressed at near histone-octamer levels and globally alters the chromatin state. Mol. Cell *37*, 457–468.

Su, Z.D., Niu, W.Z., Liu, M.L., Zou, Y.H., and Zhang, C.L. (2014). In vivo conversion of astrocytes to neurons in the injured adult spinal cord. Nat. Commun. *5*, 3338.

Tang, X., Zhou, L., Wagner, A.M., Marchetto, M.C.N., Muotri, A.R., Gage, F.H., and Chen, G. (2013). Astroglial cells regulate the developmental timeline of human neurons differentiated from induced pluripotent stem cells. Stem Cell Res. *11*, 743–757.

Torper, O., Ottosson, D.R., Pereira, M., Lau, S., Cardoso, T., Grealish, S., and Parmar, M. (2015). In vivo reprogramming of striatal NG2 Glia into functional neurons that integrate into local host circuitry. Cell Rep. *12*, 474–481.

Urban, N., and Guillemot, F. (2014). Neurogenesis in the embryonic and adult brain: same regulators, different roles. Front. Cell Neurosci. *8*, 396.

Verrecchia, F., Chu, M.L., and Mauviel, A. (2001). Identification of novel TGF-beta/Smad gene targets in dermal fibroblasts using a combined cDNA microarray/promoter transactivation approach. J. Biol. Chem. *276*, 17058–17062.

Yang, N., Ng, Y.H., Pang, Z.P.P., Sudhof, T.C., and Wernig, M. (2011). Induced neuronal cells: how to make and define a neuron. Cell Stem Cell *9*, 517–525.

Yiu, G., and He, Z. (2006). Glial inhibition of CNS axon regeneration. Nat. Rev. Neurosci. *7*, 617–627.

Zhang, L., Yang, X.Y., Yang, S.Y., and Zhang, J.N. (2011). The Wnt/beta-catenin signaling pathway in the adult neurogenesis. Eur. J. Neurosci. *33*, 1–8.

Zhang, L., Yin, J.C., Yeh, H., Ma, N.X., Lee, G., Chen, X.A., Wang, Y.M., Lin, L., Chen, L., Jin, P., et al. (2015). Small molecules efficiently reprogram human astroglial cells into functional neurons. Cell Stem Cell *17*, 735–747.

Zhang, M.L., Lin, Y.H., Sun, Y.J., Zhu, S.Y., Zheng, J.S., Liu, K., Cao, N., Li, K., Huang, Y.D., and Ding, S. (2016a). Pharmacological reprogramming of fibroblasts into neural stem cells by signaling-directed transcriptional activation. Cell Stem Cell *18*, 653–667.

Zhang, Y., Sloan, S.A., Clarke, L.E., Caneda, C., Plaza, C.A., Blumenthal, P.D., Vogel, H., Steinberg, G.K., Edwards, M.S.B., Li, G., et al. (2016b). Purification and characterization of progenitor and mature HA reveals transcriptional and functional differences with mouse. Neuron *89*, 37–53.

Zhao, Y., Zhao, T., Guan, J., Zhang, X., Fu, Y., Ye, J., Zhu, J., Meng, G., Ge, J., Yang, S., et al. (2015). A XEN-like state bridges somatic cells to pluripotency during chemical reprogramming. Cell *163*, 1678–1691.

Stem Cell Reports, Volume *12*

Supplemental Information

Chemical Conversion of Human Fetal Astrocytes into Neurons through Modulation of Multiple Signaling Pathways

Jiu-Chao Yin, Lei Zhang, Ning-Xin Ma, Yue Wang, Grace Lee, Xiao-Yi Hou, Zhuo-Fan Lei, Feng-Yu Zhang, Feng-Ping Dong, Gang-Yi Wu, and Gong Chen

Supplemental figures and legends:

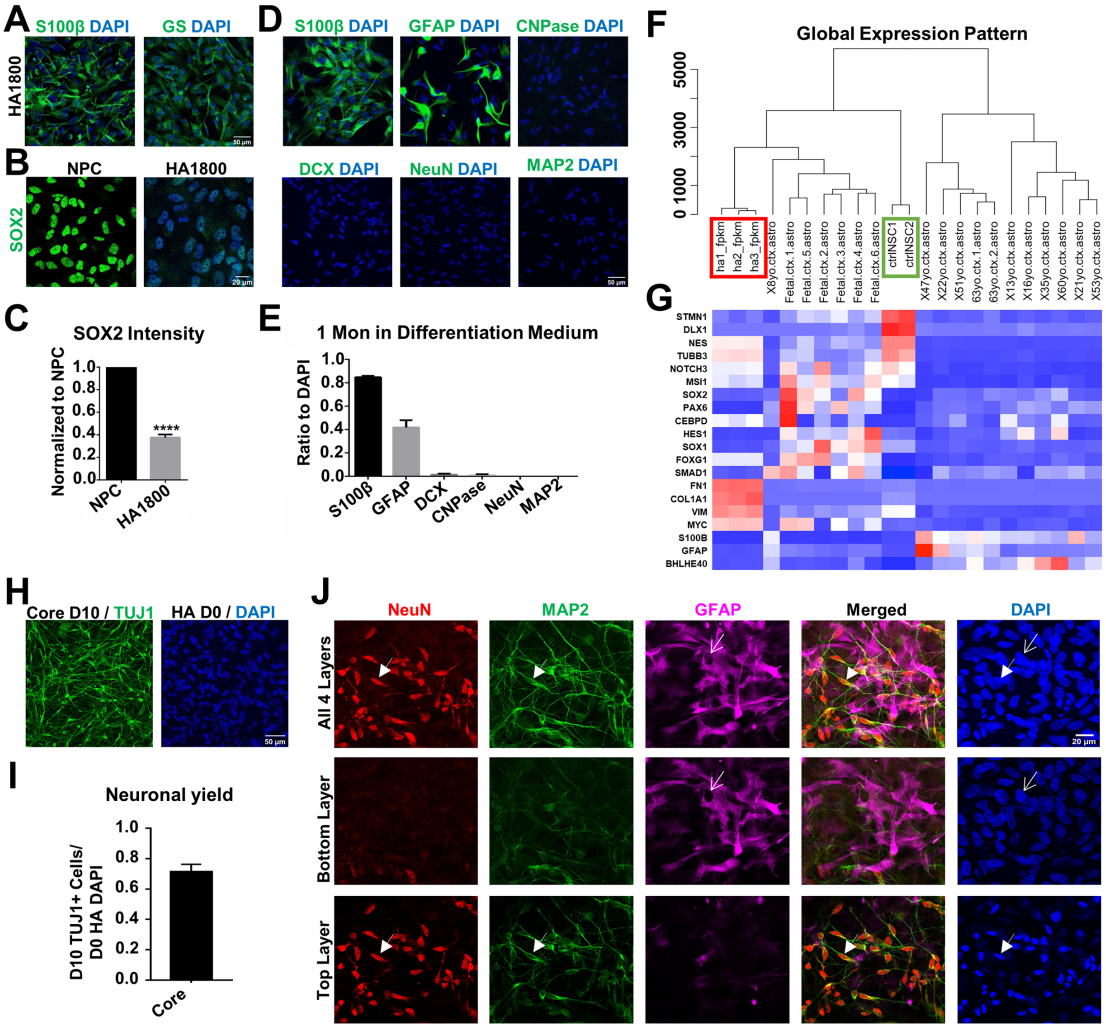

Figure S1. Characterization of human cortical astrocytes, neuronal yield, and neuron-astrocyte co-cultures after conversion. Related to Figure 1.

(A) Human astrocytes (HA1800, ScienCell) are immunopositive for astrocyte markers S100β and glutamine synthetase (GS).

(B-C) Human astrocytes are different from neuroprogenitor cells (NPCs). Immunostaining of stem cell marker SOX2 on NPCs and HA1800. Quantitative analysis showed much lower expression of SOX2 in human astrocytes than in NPCs. ****p< 0.0001, unpaired *t* test. Data are represented in mean + SEM. N = 3 batches.

(D-E) No neural differentiation in human astrocyte cultures. Human astrocytes were cultured in differentiation medium for 1 month, and then immunostained with astrocyte markers S100β, GFAP, new born neuron marker doublecortin (DCX), mature neuronal marker NeuN and MAP2, and oligodendrocyte marker CNPase (D). The number of each marker was quantified and the ratio to DAPI was calculated. After one month of culture, 83 ± 1% of cells had S100β signal, while 42 ± 6% were labelled by GFAP. Very few cells were found positive for neuronal markers or oligodendrocyte marker (E). Data are represented in mean + SEM. N = 3 batches.

(F) Dendrogram of sample relationship based on global gene expression profiles. Our human astrocytes (red box) are more similar to human fetal astrocytes as reported before than human neural stem cell (green box) or human adult astrocytes. The datasets used for comparison are from previous studies (Modrek et al., 2017; Zhang et al., 2016b).

(G) Different expression profiles of some typical cell markers among human astrocytes and NSCs.

(H-I) Neuronal yield after core drug-induced neuron conversion. Immunostaining of neuronal marker TUJ1 was performed 10 days after initial drug treatment (H). Neuronal yield after core drug treatment (I, 71.3 ± 5.0%) was calculated as the number of TUJ1+ neurons divided by the number of initial human astrocytes (DAPI staining for cell count). N = 3 batches.

(J) Converted neurons and non-converted astrocytes form a nice co-culture system. 14 days after the initiation of drug treatment, we performed immunostaining with astrocyte marker GFAP (magenta) and neuronal markers NeuN (red) and MAP2 (green). Multiple layers of Z-stack images were taken using a Zeiss confocal microscope. The upper panel showed projected images of all four layers. Bottom layer showed mostly GFAP signals (open arrow) but few NeuN or MAP2 signal. Top layer showed mainly NeuN and MAP2 signal (solid arrow) but little GFAP signal, suggesting that neurons were on top of astrocytes after conversion. N = 3 batches.

Scale bars: A, D, H, 50 μm; B and J, 20 μm.

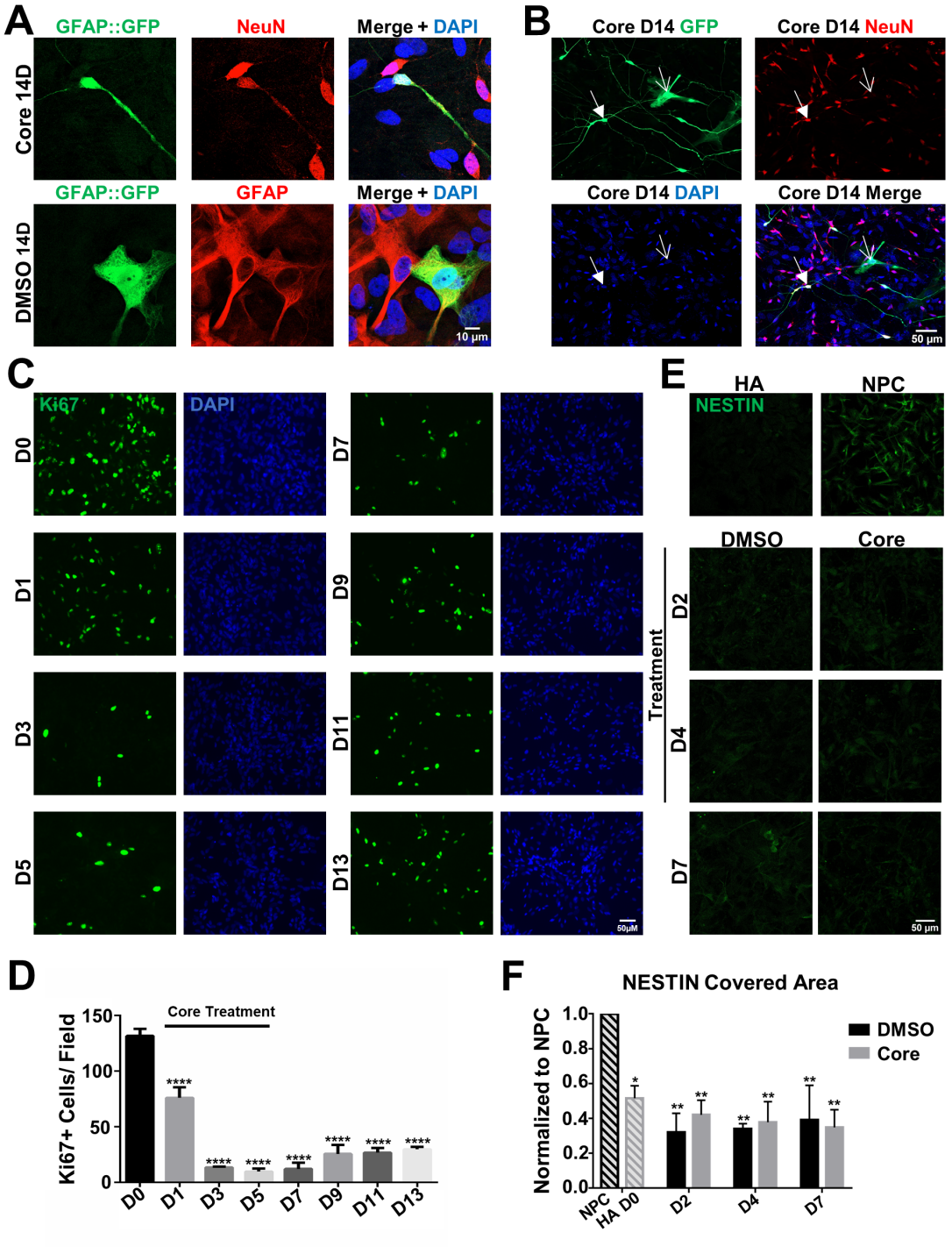

Figure S2. Core drugs directly convert human astrocytes into neurons. Related to Figure 1.

(A) Lineage tracing illustrates direct astrocyte-to-neuron conversion. Human astrocytes were infected with GFAP::GFP retrovirus for lineage tracing. Cells were then treated with either DMSO or Core drugs for 6 days. 14 days after initial drug treatment, immunostaining of GFP (Green), GFAP (Red) and NeuN (Red) were performed. In DMSO control group (Lower panel), GFP+ cells were GFAP+ astrocytes; while in core drug group (Upper panel), GFP+ cells were converted into NeuN+ neurons. N = 3 batches.

(B) Immunostaining after time-lapse imaging (see supplementary Movie S1) revealed that the majority of GFP-labeled cells with long processes were NeuN-positive neurons (labeled by solid arrow), while open arrow indicates a cell that stayed as astrocyte morphology. N = 3 batches.

(C-D) Assessment of cell proliferation after drug treatment. Human astrocytes were treated with core drugs from D1-D6. Immunostaining of cell proliferation marker Ki67 was performed before (D0), during (D1, D3, D5) and after (D7, D9, D11 and D13) drug treatment (C). Quantification of cell proliferation changes after core drug treatment. Ki67 positive cells were quantified in each 20x field. Cell proliferation rate significantly decreased during core drug treatment compared to D0 before drug application. A slight increase of cell proliferation was observed after drug removal (D). ****$p < 0.0001$, One-way ANOVA, Dunnett's multiple comparisons test. Data are represented as mean + SEM. N = 3 batches.

(E-F) No progenitor cells generated during core drug treatment. DMSO and core drugs were applied to human astrocytes from D1 to D6. Neuroprogenitor cell marker NESTIN signal (E, Green) was monitored before, during (D2, D4), and after DMSO or core treatment (D7). Statistical analyses showed a significant difference of NESTIN signal between neuroprogenitor cells (NPC) and all human astrocyte groups, whether treated with DMSO or core drugs (F). Two-way ANOVA followed by Dunnett's multiple comparisons test. *$p < 0.05$, **$p < 0.01$. Data are represented in mean + SEM. N = 3 batches.

Scale bars: A, 10 μm; B, C, E, 50 μm.

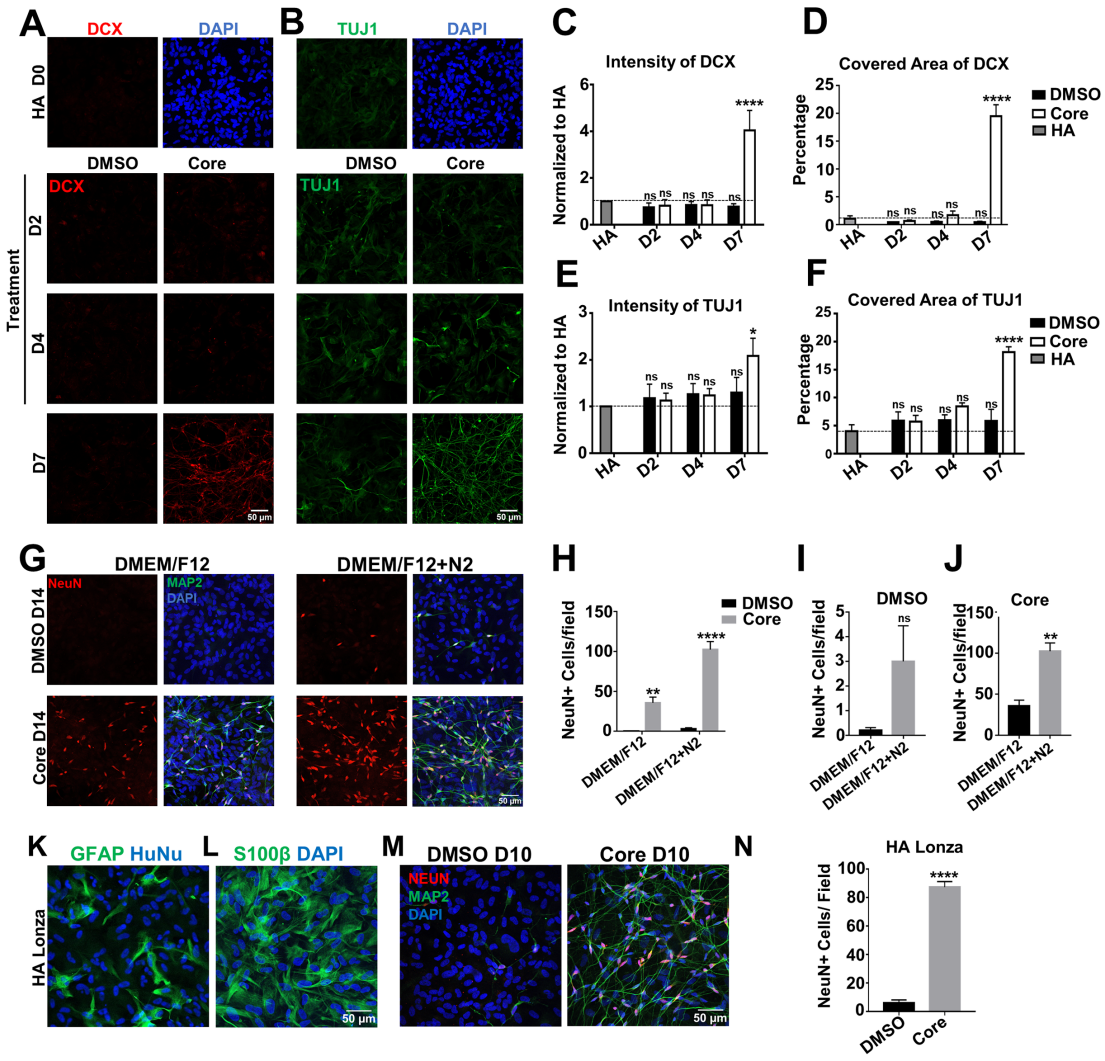

Figure S3. Further characterization of early conversion process. Related to Figure 1.

(A-F) Investigation of chemical conversion during early days using immature neuronal markers. DCX (A, red) and TUJ1 (B, green) immunostaining was performed before (D0), during (D2, D4) and after DMSO or core treatment (D7), to monitor newborn neurons (A-B). Statistical analyses of DCX signal (C-D) or TUJ1 signal (E-F) showed no change in DMSO control group, but a dramatic increase in core drug group at D7. Two-way ANOVA followed by Dunnett's multiple comparisons test. *p< 0.05, ****p< 0.0001. Data are represented in mean + SEM. N = 3 batches.

(G-J) N2 has a weak neural induction effect. DMSO or Core drugs were applied to human astrocytes in culture medium either with DMEM/F12 alone or DMEM/F12 + N2 supplement. Immunofluorescent staining of neuronal markers NeuN (G, red) and MAP2 (G, green) was performed at day 14. The number of NeuN+ cells was quantified in each field. In both medium, core drug group showed a large number of NeuN+ cells, which was significantly different from DMSO group (H). DMSO control group with DMEM/F12 alone produced almost no NeuN+ cells, while DMEM/F12 + N2 supplement showed ~3 NeuN+ cells in each field (I), suggesting a weak neural induction effect of N2 supplement. Core drugs in DMEM/F12 + N2 medium also induced more neurons from human astrocytes, compared to that in DMEM/F12 alone (J). Two-way ANOVA followed by Sidak's multiple comparisons test. **p< 0.01, ****p< 0.0001. Data are represented in mean + SEM. N = 3 batches.

(K-L) Human astrocytes purchased from Lonza were characterized by human nuclei marker HuNu (K, Blue), and astrocyte markers GFAP (K, Green) and S100β (L, Green).

(M-N) Chemical conversion of Lonza astrocytes into neurons after core drug treatment. Core drugs (2.5 μM SB431542, 0.125 μM LDN193189, 0.75 μM CHIR99021 and 2.5 μM DAPT) or 0.1% DMSO were added to Lonza astrocytes for 4 days, then replaced by neuronal differentiation medium. Immunohistochemistry of neuronal markers NeuN (M, red) and MAP2 (M, green) was performed 10 days after initial drug treatment. Core drug group showed a large number of neurons compared to the control group (N). ****$p < 0.0001$, unpaired *t* test. Data are represented in mean + SEM. N = 3 batches.

Scale bars: A, B, G, K, L, M, 50 μm.

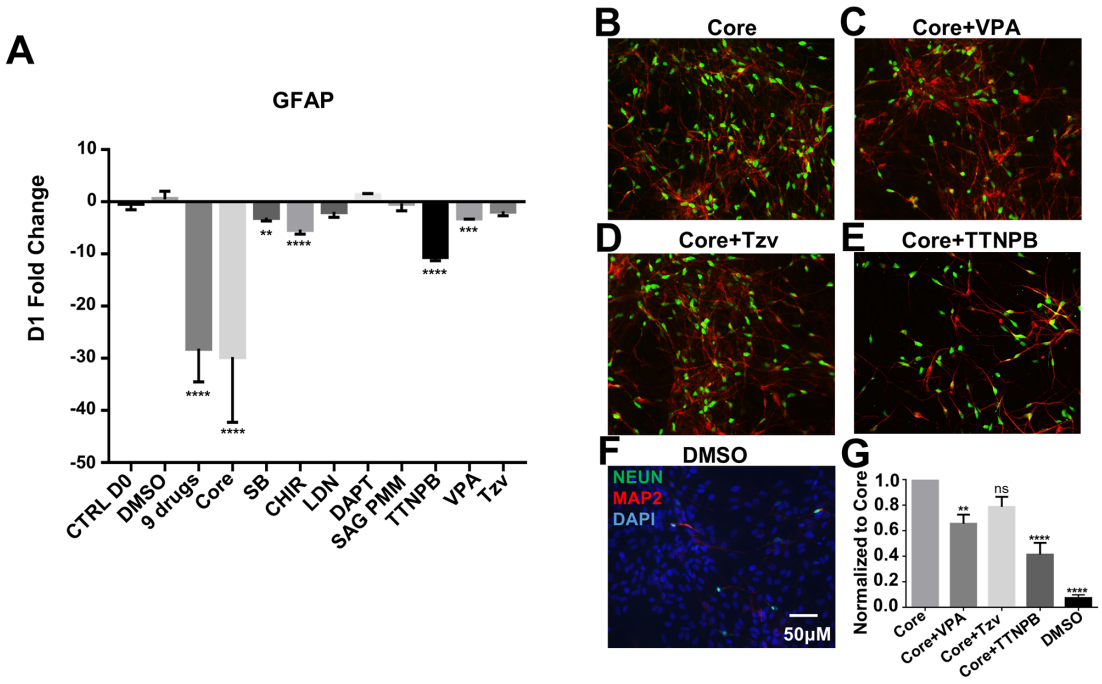

Figure S4. Downregulation of glial genes by small molecules. Related to Figure 2.

(A) Quantitative real-time PCR analyses showed a significant downregulation of GFAP in human astrocytes after 1-day core drug treatment. GFAP was dramatically downregulated by both 9 drugs and core drugs. Among individual drugs, SB431542, CHIR99021, TTNPB and VPA also significantly decreased GFAP. **p < 0.01, ***p < 0.001, ****p< 0.0001, One-way ANOVA after $\log_2$ transformation, Dunnett's multiple comparison test. Data are represented in mean + SEM. N = 3 batches.

(B-F) Addition of extra drugs did not improve conversion efficiency. Human astrocytes were treated with core drugs (B), core drugs plus 0.1 mM VPA (C), or 0.5 μM Tzv (D), or 0.5 μM TTNPB (E) for 6 days. 0.2% DMSO (F) served as control group. Immunostaining of NeuN (green) and MAP2 (red) was performed at day 14 after the initiation of drug treatment. Scale bar: B-F, 50 μm.

(G) Quantified data showing a decrease of conversion efficiency after addition of drugs to the core-drug formula. The number of NeuN-positive cells in each field was quantified, and each group was normalized to the core drug group. The addition of Tzv did not change the reprogramming efficiency, while VPA and TTNPB both decreased the reprogramming efficiency. **p < 0.01, ****p< 0.0001, One-way ANOVA, Dunnett's multiple comparisons test. Data are represented in mean + SEM. N = 3 batches.

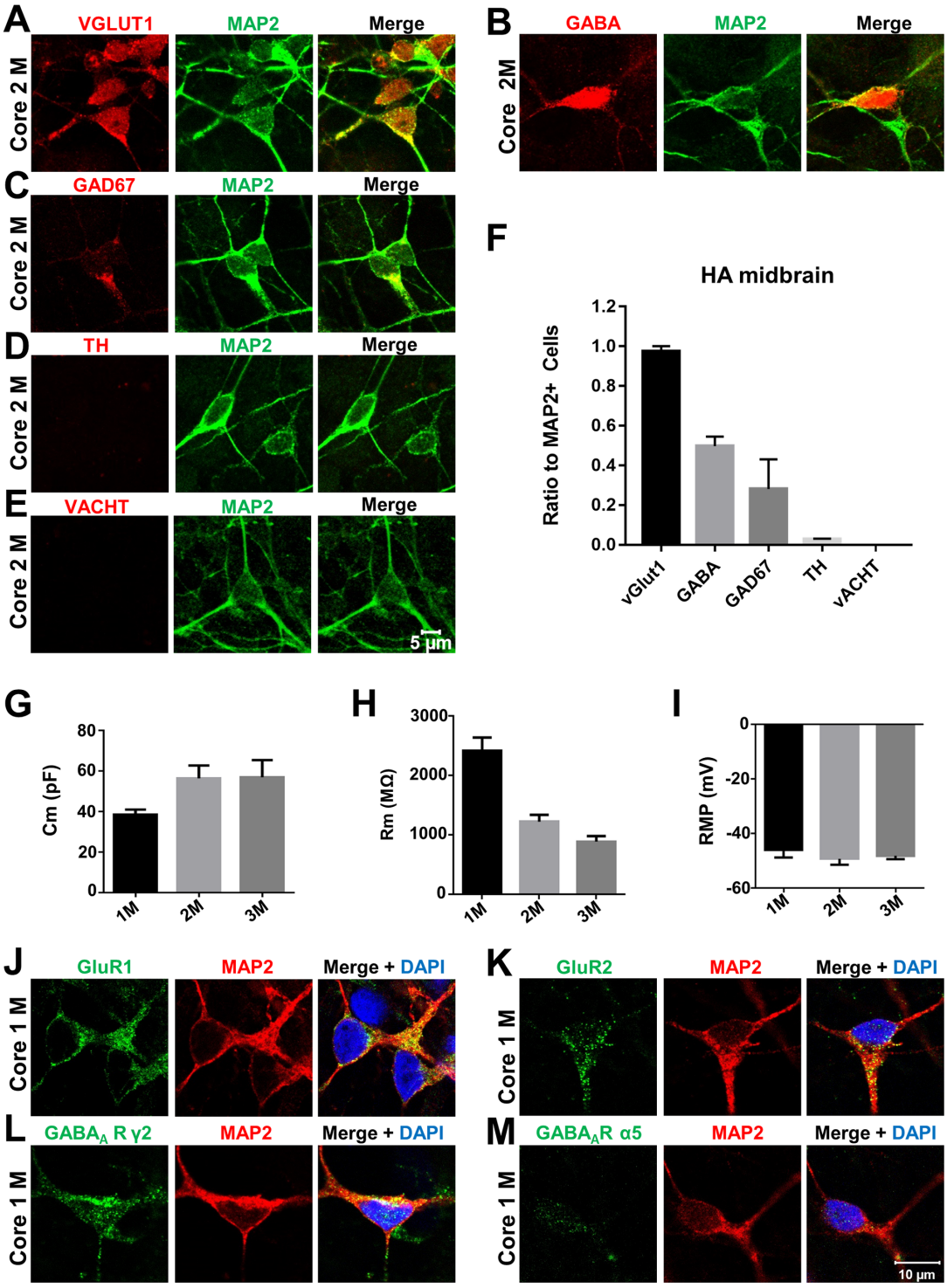

Figure S5. Some GABAergic neurons are induced from human midbrain astrocytes by core drugs. Related to Figure 3 and Figure 4.

(A-F) Core drug-induced chemical conversion in human midbrain astrocytes. Human midbrain astrocytes (ScienCell) were treated with core drugs for 6 days and then cultured for 2 months. Immunostaining of different neuronal subtype markers was performed. Human midbrain astrocyte-converted neurons (MAP2,

green) induced by core drugs were mainly glutamatergic (A, VGlut1, red, 97.4 ± 2.6%). Interestingly, some iNs also showed GABAergic neuron markers, such as GABA (B, red, 49.8 ± 4.7%) or GAD67 (C, red, 28.1 ± 15.0%), but dopaminergic (D, TH, Red, 2.8 ± 1.7%) or cholinergic neurons (E, VACHT, RED, 0%) were rarely detected. F, quantified data showing different subtypes of neurons after core drug treatment. Quantitative data were represented in mean + SEM (F). N = 3 batches.

(G-I) Developmental change of membrane capacitance (Cm, G), membrane resistance (Rm, H), and resting membrane potential (RMP, I) of core drug-induced neurons from 1 month to 3 months cultures. Data were represented by mean + SEM. N > 30 in each group.

(J-M) 1 month after core treatment, converted neurons (MAP2, red) expressed both glutamate receptors, shown by immunostaining of GluR1 (J, green) and GluR2 (K, green) subunits, and $GABA_A$ receptors shown by immunostaining of γ2 (L, green) and α5 subunits (M, green). N = 3 batches.

Scale bars: A-E, 5 μm; J-M, 10 μm.

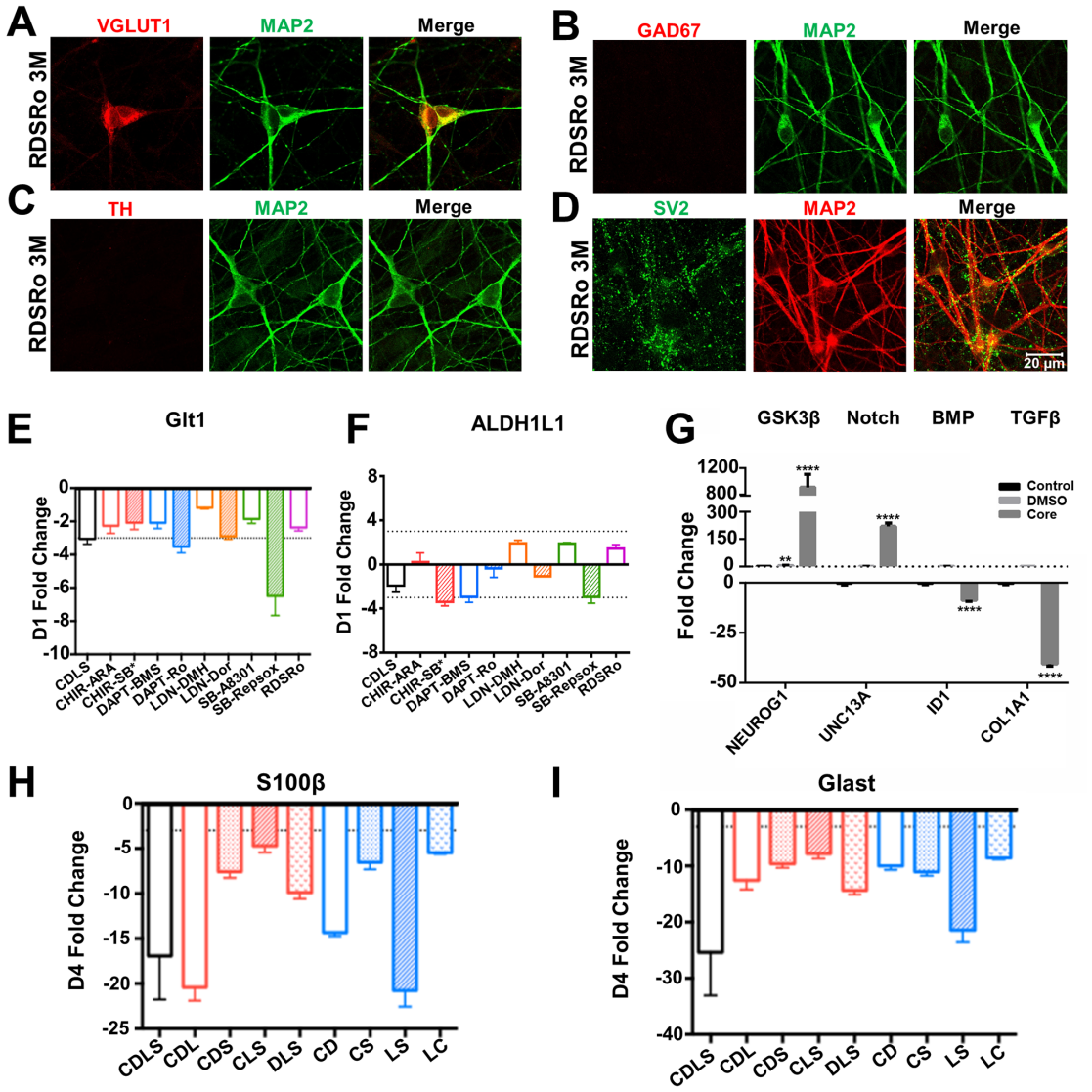

Figure S6. Chemical conversion mediated by various combinations of small molecules. Related to Figure 5 and Figure 6.

(A-C) The functional analogs of core drugs also converted human astrocytes (HA1800, ScienCell) into glutamatergic neurons. At 3 months after treatment with functional analogs including Repsox, Dorsomorphin, SB216763 and RO4929097 (RDSRo), most iNs showed vGlut1 signal (A, red), but not GAD67 (B, red) or TH signal (C, red). N = 3 batches.

(D) Three months after treatment with functional analogs (RDSRo), a large number of synaptic puncta (SV2, green) were found along MAP2-labelled dendrites (red). N = 3 bathes. Scale bar: A-D, 20 μm.

(E-F) Downregulation of glial genes by functional analogs of core drugs. After 1-day treatment of core drugs or core drugs replaced by their functional analogues, real-time PCR analysis showed a decrease of astrocyte marker Glt1 (E) and mildly of ALDH1L1 (F). Dash line indicates 3-fold change. All data was normalized to D1 DMSO control group. Data are represented in mean + SEM. N = 3 batches.

(G) Signaling pathways affected by core drugs during reprogramming. Human astrocytes were treated with core drugs for 4 days, then collected for RT-PCR experiments. The expression of NEUROG1 is the direct

target of β-catenin in GSK3β-mediated pathway. UNC13A is the direct target of Notch pathway effector NICD. ID1 is the target gene of BMP pathway. COL1A1 is the target gene of TGFβ pathway. **p < 0.01, ****p< 0.0001, One-way ANOVA after $\log_2$ transformation, Dunnett's multiple comparisons test. Data are represented in mean + SEM. N = 3 batches.

(H-I) Downregulation of glial genes by 3 or 2 small molecules. Human astrocytes were treated with 4 core drugs (CDLS), 3-drug combinations (CDL, CDS, CLS, DLS) and 2-drug combinations (CD, CS, LS, LC). Real-time PCR analysis was performed on these drug combinations at D4 to analyze astrocytic markers S100β and Glast expression. All groups showed downregulation of S100β and Glast, compared to D0 human astrocytes. Dash line indicates 3-fold change. N = 3 batches.

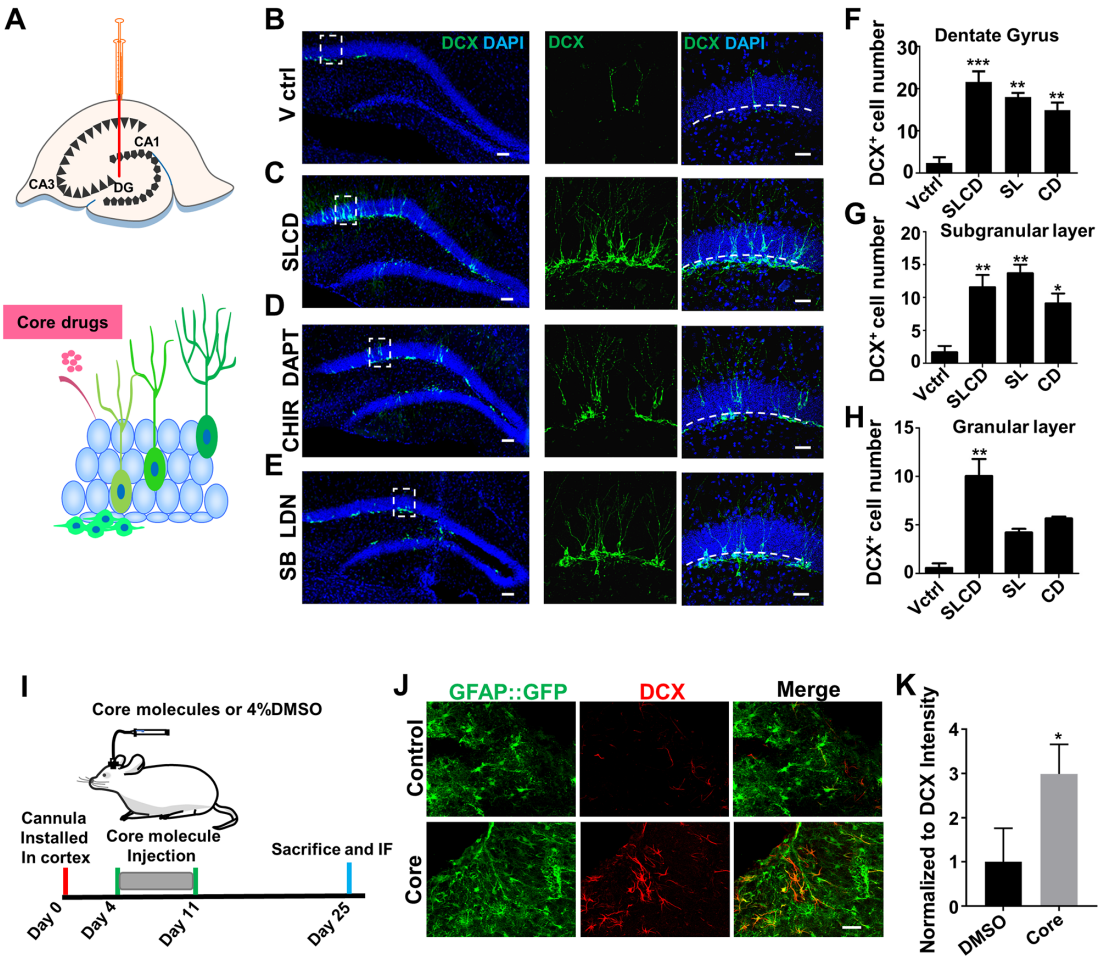

Figure S7. Core drugs increased hippocampal neurogenesis and DCX+ cells in the cortex *in vivo*. Related to Figure 7.

(A) Illustration of a single dose of drug injection into the dentate gyrus of mouse brains. After 7 days, the mice were sacrificed for immunostaining.

(B) When 4% DMSO was injected into the hippocampus of 1-year-old mouse, very few DCX+ newborn neurons were detected in the hippocampus.
(C-E) Injection of small molecules into the dentate gyrus with core drugs (C) (SB431542 50μM, LDN193189 5 μM, CHIR99021 15 μM, DAPT 50 μM), or only two drugs of CHIR99021 + DAPT (D), or SB431542 + LDN99021 (E) significantly increased the DCX+ cell number in the subgranular layer (under the dash line) and granular layer (above dash line). Scale bars for B-E: left panel in low magnification, 60 μm; right panels in high magnification, 30 μm.
(F-H) Quantitative analysis revealed a significant increase of DCX+ cell number induced by small molecules in the entire dentate gyrus (F), or subgranular layer (G) and granular layer (H). * $P < 0.01$, ** $P < 0.001$, *** $P < 0.0001$, one-way ANOVA followed by Dunnett's test. N = 3 mice for each group.

(I) Schematic illustration of intracranial administration of small molecules through mini-osmotic pump. Brain cannula was installed in GFAP::GFP mouse cortex, where astrocytes were labeled green. Core drugs including SB431542 50 μM, LDN193189 5 μM, CHIR99021 15 μM, and DAPT 50 μM in a total volume of 100 μl were perfused through mini-osmotic pump (Alzet, Cupertino, CA) for 7 days. In control mice, 4% DMSO was perfused as vehicle control. Mice received small molecules were sacrificed for

immunostaining 2 weeks after small molecule treatment.
(J-K) Representative images (J) and quantitative analysis (K) revealed an increased DCX expression in GFAP-expressing reactive astrocytes. No neuronal morphology was observed. N = 3 mice, Student t test * $P< 0.05$, Scale bar for J, 30 μm.

Supplemental tables:

Table S1. Antibodies used for Immunostaining. Related to Figure 1-7 and Figure S1-S7.

polyclonal anti-NEUN	rabbit, 1:1000, Millipore, ABN78
polyclonal anti-Microtubule Associated Protein 2 (MAP2)	chicken, 1:2000, Abcam, AB5392
monoclonal anti-βIII tubulin (TUJ1)	mouse, 1:1000, COVANCE, MMS-435P
polyclonal anti-MECP2	rabbit, 1: 500, Diagennode, 15410052
polyclonal anti-REST	rabbit, 1:600, Sigma, SAB2108706
polyclonal anti-T-box, brain, 1 (TBR1)	rabbit, 1: 300, Abcam, AB31940
polyclonal anti-PROX1	rabbit, 1:1000, ReliaTech GmbH, 102-PA32
monoclonal anti-CTIP2	rat, 1:600, Abcam, ab18465
anti-HOXB4	mouse, 1:200, Developmental Studies Hybridoma Bank, Iowa City, I12 anti Hoxb4
polyclonal anti-vesicular glutamate transporter 1 (VGLUT1)	rabbit, 1:1000, Synaptic Systems
monoclonal anti-GAD67	mouse, 1:1000 Millipore, MAB5406
monoclonal anti tyrosine hydroxylase (TH)	mouse, 1:600, Millipore, MAB318
polyclonal anti-vesicular glutamate transporter (SV2)	mouse, 1:1000, Developmental Studies Hybridoma Bank, Iowa City
polyclonal anti-green fluorescent protein (GFP)	chicken, 1:1000, Abcam, AB13970
polyclonal anti-glial fibrillary acidic protein (GFAP)	chicken, 1:1000, Millipore, AB5541
polyclonal anti-glial fibrillary acidic protein (GFAP)	Rabbit, 1:1000, Millipore, AB5804
monoclonal anti-Human Nuclei (HuNu)	mouse, 1:1000, Millipore, MAB1281
polyclonal anti-CDP (CUX1)	rabbit, 1:500, Santa Cruz, SC-13024
polyclonal anti-NURR1	rabbit, 1:2000, Santa Cruz, SC-991
monoclonal anti-S100β	mouse, 1:800, Abcam, ab66028
monoclonal anti-Glutamine Synthetase (GS)	mouse, 1:800, Millipore, MAB302
monoclonal anti-CNPase	mouse, 1:800, Abcam, ab6319
polyclonal anti-Doublecortin (DCX)	rabbit, 1:500, Abcam, AB18723
polyclonal anti-Doublecortin (DCX)	goat, 1:500, Santa Cruz, sc-8066
polyclonal anti-SOX2	rabbit, 1:800, Millipore, AB5603
polyclonal anti-Ki67	rabbit, 1:800, Abcam, ab15580
Monoclonal anti-BrdU	rat, 1:1000, Accurate, OBT0030
Monoclonal anti-GluR1	mouse, 1:800, Millipore, MAB2263
Monoclonal anti-GluR2	mouse, 1:800, Millipore, MAB397
Polyclonal anti-$GABA_A$ receptor α5 subunit	rabbit, 1:800, abcam, ab10098
Polyclonal anti-$GABA_A$ receptor γ2 subunit	Rabbit, 1:800, SYSY, 224003

Table S2. Sequences of primers used in RT-PCR. Related to Figure 2, 3 & Figure S4, S6.

NGN2-F	ATTTGCAATGGCTGGCATCT
NGN2-R	CACAGCCTGCAGACAGCAAT
NEUROD1-F	CCTGCAACTCAATCCTCGGA
NEUROD1-R	GGCATGTCCTGGTTCTGCTC
GAPDH-F	TGGGCTACACTGAGCACCAG
GAPDH-R	GGGTGTCGCTGTTGAAGTCA
PROX1-F	GCCAAACTCCTTACAACCGGA
PROX1-R	GGCCGAAAAGACTTTGACCAC
CTIP2-F	ACCTGTGGCCAGTGTCAAATG
CTIP2-R	TTGTCATAGCAGGCACCCAAG
TBR1-F	TGGATGTGATTTTGGCGGA
TBR1-R	CCGGATGCATATAGACCCGAT
CUX1-F	ATGCCACCGCAACGGTATT
CUX1-R	GCGCAAATCCTCTGGAGTGTT
NURR1-F	AATGCGTTCGTGGCTTTGG
NURR1-R	AGCAATGCAGGAGAAGGCAGA
HOXB4-F	ACGGTAAACCCCAATTACGCC
HOXB4-F	TTTTCCACTTCATGCGCCG
NEUN-F	GCCCCGCTCGTTAAAAATG
NEUN-R	ACACGTCTCCAACATCCCCTT
NEUROG1-F	ACCGCATGCACAACTTGAAC
NEUROG1-R	ATGTAGTTGTAGGCGAAGCGC
UNC13A-F	CTTTGTACAGACGCAATCGGC
UNC13A-R	TGTGTTCCCCAGTTCCTGGAT
ID1-F	CGTGCTGCTCTACGACATGAA
ID1-R	TGCTGGAGAATCTCCACCTTG
COL1A1-F	AATCACCTGCGTACAGAACGG
COL1A1-R	CAGATCACGTCATCGCACAAC
GFAP-F	CGCAGTATGAGGCAATGGC
GFAP-R	ACCACTCTTCGGCTTCATGC
Glt1-F	CCAGGAAAAACCCCTTCTCCT
Glt1-R	CAACGAAAGGTGACAGGCAAA
ALDH1L1-F	CGCTGTACAACCGCTTCCTC
ALDH1L1-R	CCTGCACCATCCCTTTGATG
S100β-F	CCGAACTGAAGGAGCTCATCA
S100β-R	CATTCGCCGTCTCCATCATT
Glast-F	AGAACAATGGCGTGGACAAGC
Glast-R	AATGGCAGCCAAAGCCTCAT

Supplemental Experimental Procedures:

Time-lapse imaging

Human astrocytes were infected with CAG::GFP lentivirus in order to visualize the morphological change of astrocytes during and after drug treatment (Zhang et al., 2015). When the cells reached ~90% confluence, core drugs (5 μM SB431542, 0.25 μM LDN193189, 1.5 μM CHIR99021 and 5 μM DAPT) were added into N2 medium to reprogram human astrocytes, some of which were GFP-labeled after lentiviral infection. The cells were then put into the IncuCyte system (Essen BioScience, Ann Arbor, Michigan) for four continuous days without any medium change. Images were taken every two hours to trace the morphology change of human astrocytes. Drugs were withdrawn after four days and neuronal differentiation medium was added to the cells. Image taking was conducted until eight days, when most converted cells showed neuronal processes.

Immunocytochemistry

Cells on coverslips were fixed in 4% PFA (Alfa Aesar) at room temperature for 12 min, and then PFA was washed off with PBS for three times. After washing, coverslips were transferred into blocking buffer, and incubated on the shaker in a slow speed for 1 hr. The blocking buffer was made of 2.5% normal donkey serum (Jackson ImmunoResearch), 2.5% normal goat serum (Jackson ImmunoResearch), 0.1% Triton X-100 (Fisher Scientific) in PBS. After blocking, cells were incubated in primary antibodies overnight at 4 ℃. The second day, primary antibodies were washed off with PBS for three times. Then, cells were incubated in corresponding secondary antibodies for 1 hr in room temperature. Secondary antibodies were tagged with fluorophore Alexa Fluor 488, Alexa 594, Alexa 647 (1:800, Molecular Probes). After incubation, secondary antibodies were washed off with PBS for three times. Coverslips with cells were finally mounted on glass slides with mounting solution containing DAPI (Invitrogen). Triton was removed from blocking buffer for the staining of glutamate and GABA receptors. The immunostaining results were analyzed using fluorescent microscopes (Nikon ECLIPSE TE2000-S and ZEISS ApoTome). Confocal microscopes (Olympus FV1000 and ZEISS LSM800) were also used to take images. Antibodies were listed in Table S1.

Electrophysiology

Multiclamp 700A patch-clamp amplifier (Molecular Devices, Palo Alto, CA) was used to perform whole-cell recordings. Coverslips with converted iNs were transferred into a recording chamber, which was constantly perfused with bath solution containing 128 mM NaCl, 30 mM glucose, 25 mM HEPES, 5 mM KCl, 2 mM Ca^{2+}, and 1 mM $MgCl_2$. The pH of bath solution was adjusted to 7.3 with NaOH, and osmolality was 300-305 mOsm/L. The pipette solution consisted of 135 mM KCl, 5 mM Na-phosphocreatine, 10 mM HEPES, 2 mM EGTA, 4 mM Mg-ATP, and 0.5 mM Na_2GTP. The pH of pipette solution was adjusted to 7.3 with KOH, and osmolality to 280-290 mOsm/L. Patch pipettes were pulled from borosilicate glass, and the pipette resistance was 3-6 MΩ after filled with pipette solution. The series resistance after forming whole-cell recording was under 25 MΩ and not compensated during recording to reduce noise. For detecting spontaneous events and sodium and potassium currents, the membrane potential was held at -70 mV under voltage-clamp mode. Drug delivery was through a gravity-driven system (VC-6, Harvard Apparatus, Hamden, CT).

RNA extraction

Human astrocytes were collected 1 day or 4 days after drug treatment. The 4-drug and 9-drug treatments were applied side-by-side. Macherey-Nagel NucleoSpin® RNA kit was used to isolate RNA from human astrocytes. 350 μl lysis buffer and 3.5 μl β-mercaptoethanol were added to each well of 24-well plate, and cell lysate was collected. After passing through one NucleoSpin® filter, RNA binds to the NucleoSpin® RNA column. After DNase treatment, and three times washing, RNA was purified. The pure RNA was eluted with 40 μl RNase-free water, and RNA concentration was measured by NanoDrop. Isolated RNA was stored in -80 ℃ for reverse transcription.

Reverse transcription and RT-PCR

Quanta Biosciences qScript^{TM} cDNA SuperMix (5X) was used to synthesize cDNA from isolated RNA. 1 μg RNA template, 4 μl qScript^{TM} cDNA SuperMix was used in each reaction. RNase/DNase-free water was added to make the reaction volume 20 μl. Then the reaction mix was incubated at 25 ℃ for 5 min, 42 ℃ for 30 min, and 85 ℃ for 5 min. cDNA was diluted in RNase/DNase free water for 5 times. Quanta Biosciences PerfeCTa^{TM} SYBR® Green SuperMix, ROX^{TM} was used for RT-PCR. 5 μl cDNA was used in 25 μl reaction volume. 40 PCR cycles, each of which contained 15 s at 95 °C and 45 s at 65 °C, were performed to amplify the reaction mix. Comparative Ct values were used to calculate the gene expression fold difference. GAPDH was used as the internal control, and relative Ct values were further normalized to human astrocytes collected at D0, before drug treatment. Each sample had three replicates in each PCR reaction. All RT-PCR data was $\log_2$ transformed to fit normal distribution assumption of one-way ANOVA. Some primers were adapted from our recent 9-drug protocol (Zhang et al., 2015), and the sequences of all primers were listed in Table S2.

RNA-sequencing Analysis

After RNA extraction, the qualities of human astrocyte samples were examined on Agilent 2100 bioanalyzer at UCLA Technology Center for Genomics & Bioinformatics, followed by mRNA enrichment and library construction. Single-end 50 bp sequencing was performed on HiSeq 3000. Quality check of the raw data was done using FastQC (v. 0.11.3), then reads were aligned against human reference genome hg38 using HISAT2 (v. 2.0.1) (Kim et al., 2015) and summarized using stringtie (v. 1.3.4) (Pertea et al., 2015). Genes with FPKM < 0.1 were removed. This RNAseq data is available in Gene Expression Omnibus (GEO: GSE123397). Datasets for induced neural stem cells (GSE94962) and human fetal & adult astrocytes (GSE73721) were published by previous studies (Modrek et al., 2017; Zhang et al., 2016).

Lineage Tracing

Human astrocytes (ScienCell, 1800) cultured in 24-well plate were infected with 2 μl pGFAP::GFP-IRES-GFP retrovirus for overnight. Cells were then treated with 0.2% DMSO or small molecules. 14 days after treatment, cells were fixed for the immunostaining of neuronal markers and GFP.

Stereotaxic injection of small molecules into mouse brain

All animal studies were approved by Penn State IACUC committee and in accordance with NIH guidelines on animal welfares. Brain surgeries were performed on 2-month old wild-type C57BL6 mice. Mice were anesthetized by injecting 20 mL/kg 0.25% Avertin (a mixture of 25 mg/ml of tribromoethylethanol and 25 μl/ml T-amyl-alcohol) into the peritoneum and then placed in a stereotaxic device. Artificial eye ointment was applied to cover and protect the eye. The animals were operated with a midline scalp incision and a drilling hole on the skull above somatosensory cortex. Each mouse received one injection in the dentate gyrus (coordinates: AP -2.06 mm, ML 1.5 mm, DV -2.1 mm) of small-molecule mixture [SB431542 (0.2 mM), LDN193189 (10 μM), CHIR99021 (60 μM) and DAPT (0.2 mM)] or PBS containing 2% DMSO with a 5 μl syringe and a 34 gauge needle. The injection volume and flow rate were controlled as 2 μl at 0.2 μl/min. After injection, the needle was kept for at least 5 additional minutes and then slowly withdrawn.

Drug perfusion with mini-osmotic pump

Brain cannula was installed in GFAP::GFP mouse cortex, where astrocytes were labeled green (installation coordinate: AP 1.25 mm, ML 1.4 mm, DV -1 mm). Core drugs including SB431542 50 μM, LDN193189 5 μM, CHIR99021 15 μM, and DAPT 50 μM in a total volume of 100 μl were perfused through a mini-osmotic pump (Alzet, Cupertino, CA) for 7 days with a constant rate of 0.5 μl/hr. In control mice, 100 μl of 4% DMSO was perfused. Mice that received perfusion were sacrificed for immunostaining at 2 weeks post small molecule treatment.

Intraperitoneal injection of small molecules

Core drug cocktail including CHIR99021, 2.79 µg/10g; DAPT, 8.65 µg/10g; LDN193189, 0.55 µg/10g; SB431542, 7.69 µg/10g was injected into the peritoneum into 2-month old wildtype mice daily for 23 days. The vehicle solution (20% Captisol) was injected into WT mice (0.2ml/10g) as control. Starting from day 5, BrdU (0.1 ml/ 10 kg) was administrated every 3 to 4 days until day 26. At 32 days post the initial drug treatment, mice were sacrificed, perfused with artificial cerebral spinal fluid (ACSF). Brains were collected and post fixed in 4% paraformaldehyde. The fixed brains were washed with PBS and sectioned into 40 µm slices. Brain slices were permeabilized and blocked with 0.3% Triton, 5% normal donkey serum and incubated with primary antibodies (Rabbit anti Ki67, Goat anti DCX) at 4°C overnight. The following day, brain slices were washed with PBS and incubated with secondary antibodies (Dylight 488 Donkey anti Rabbit and Dylight 647 Donkey anti Goat). After being washed with PBS, brain slices were mounted. Images were acquired using Zeiss LSM 800 confocal microscope. Scale bar: 20 µm.

Supplemental References

Kim, D., Landmead, B., and Salzberg, S.L. (2015). HISAT: a fast spliced aligner with low memory requirements. Nat Methods *12*, 357-U121.

Pertea, M., Pertea, G.M., Antonescu, C.M., Chang, T.C., Mendell, J.T., and Salzberg, S.L. (2015). StringTie enables improved reconstruction of a transcriptome from RNA-seq reads. Nat Biotechnol *33*, 290-+.